Dynamical mesh adaption criteria for accurate capturing of stiff phenomena in combustion

Pénélope Leyland, Fayssal Benkhaldoun, Nathan Maman, Bernard Larrouturou

INRIA

INSTITUT NATIONAL DE RECHERCHE EN INFORMATIQUE ET EN AUTOMATIQUE

Dynamical mesh adaption criteria for accurate capturing of stiff phenomena in combustion

Pénélope LEYLAND
Fayssal BENKHALDOUN
Nathan MAMAN
Bernard LARROUTUROU

N° 1876
Avril 1993

PROGRAMME 6

Calcul Scientifique,
Modélisation et
Logiciels numériques

Rapport de recherche

1993

DYNAMICAL MESH ADAPTION CRITERIA FOR ACCURATE CAPTURING OF STIFF PHENOMENA IN COMBUSTION

Pénélope LEYLAND, Fayssal BENKHALDOUN
Nathan MAMAN, Bernard LARROUTUROU

Abstract

Adaptation criteria for dynamical mesh refinement algorithms aimed for simulating unsteady phenomena are studied in this paper. The applications considered here mainly concern premixed laminar flame propagation in gaseous mixtures, solved by means of a finite-element method in space and explicit time-stepping.

CRITERES POUR L'ADAPTATION DYNAMIQUE DE MAILLAGES ET APPLICATION A DES PROBLEMES DE COMBUSTION

Résumé

Nous étudions dans ce rapport les critères d'adaptation de maillage pour des algorithmes de raffinement-déraffinement dynamique. Les applications considérées concernent notamment la simulation de flammes prémélangées instationnaires en milieu gazeux, sur des maillages de type éléments finis, avec une intégration temporelle explicite.

Dynamical mesh adaptation criteria for accurate capturing of stiff phenomena in combustion

Pénélope LEYLAND, IMHEF, École Polytechnique Fédérale de Lausanne,
Écublens, 1015 LAUSANNE, SWITZERLAND.

Fayssal BENKHALDOUN, INSA - Rouen,
Place Émile Blondel, 76131 MONT SAINT AIGNAN Cedex, FRANCE.

Nathan MAMAN, INRIA,
BP 93, 06902 SOPHIA-ANTIPOLIS Cedex, FRANCE.

Bernard LARROUTUROU, CERMICS & INRIA,
BP 93, 06902 SOPHIA-ANTIPOLIS Cedex, FRANCE.

Dynamical mesh adaptation criteria for accurate capturing of stiff phenomena in combustion

Pénélope LEYLAND* Fayssal BENKHALDOUN†

Nathan MAMAN‡ Bernard LARROUTUROU§

Abstract

Adaptation criteria for dynamical mesh refinement algorithms aimed for simulating unsteady phenomena are studied in this paper. The applications considered here mainly concern premixed laminar flame propagation in gaseous mixtures, solved by means of a finite element method in space and explicit time-stepping.

Introduction

Premixed flame simulation is a particularly hard problem: the governing equations include as a sub-system a non-linear parabolic system with a high degree of stiffness coming from the very different space and time scales. In particular, the reaction takes place within a zone with a characteristic width ten times smaller than the typical flame thickness, which itself is very small compared to the global domain dimensions.

*IMHEF, École Polytechnique Fédérale de Lausanne, Écublens, 1015 Lausanne, SWITZERLAND

†INSA - Rouen, Place Émile Blondel, 76131 Mont Saint Aignan Cedex, FRANCE

‡INRIA, BP 93, 06902 Sophia-Antipolis Cedex, FRANCE

§CERMICS & INRIA, BP 93, 06902 Sophia-Antipolis Cedex, FRANCE

A sufficient density of mesh points within these zones is required to calculate the flame accurately enough and hence to obtain a correct physical behaviour. Indeed, if a too coarse mesh is used, in comparison with the typical flame thickness, the variables will be averaged in the sharp gradients regions, which may result in a false flame speed, or may even extinguish the flame.

Moreover, the flame propagates through a gas, and there exists a coupling between the combustion process and the underlying hydrodynamics, the latter having again different characteristic time and length scales.

1 Motivation and "The state of the art"

An efficient resolution of this kind of unsteady problems can be done by using the possibilities offered by the techniques of local refinement of unstructured meshes, for example triangulations in two dimensions or tetrahedrisations in three dimensions. Then, treated by a refinement/unrefinement procedure, these adapted meshes can follow the flame front, allowing convergence acceleration and greater accuracy.

In order to do this, we extract from the modelisation and the approximation method a function, called the *criterion*, which indicates at each time level t the regions where greater accuracy is required: discontinuities, high gradients, preheating regions, reaction zones, etc. Also, at least in principle, this function should be able to detect weaker secondary wave formation.

The mesh is thus locally refined in these zones, and as soon as for some $t' > t$ this function indicates that the flame has moved, the previously refined regions of the mesh now useless are coarsened and new ones may be refined, and so on. In this way several time steps may be performed on the same mesh, the criterion representing the key indication in this process.

1.1 Finite element mesh adaptation methods

Appropriate algorithms to obtain this iterative remeshing are independent of the problem under consideration, but the criterion is very closely related to it. The algorithm developed here is based upon a multiple level hierarchical data tree structure, such as those used in multigrid methods,(see e.g. [7], [8],

[39]), and multigrid methods based on adaptive, non necessarily embedded/ nested grids ([2], [6], [29], etc.)

Internal flagging simplifies the structure of the algorithm, which renders a mesh that can be read by the solver in an usual direct way using connectivity tables, global numbering sequences, etc. This adaptive procedure is called ADAPT. From a solution calculated at time step t^n by a suitable SOLVER for the problem to handle, a decision is made on whether the error requirements are acceptable or not, thus whether refinement or unrefinement is necessary or not.

This decision, made from the criteria, is used to fill an array, IADIV, taken on the current set of elements, which defines for each element the required degree m of adaptation, and the procedure ADAPT is then called. After rearrangement, renumbering and recalculation of the metrics, a new mesh is obtained, and the next solution at time level t^{n+1} can be calculated on this new mesh. Several time steps may be performed on this new mesh before the next adaptation.

1.2 Criteria

In general, one could define a good criterion as one which allows us to generate a smooth enough optimal mesh. It must take into account the unsteady nature of the problem and the stiffness coming from disparate scales.

In general we may divide error estimates for finite-element meshes into three classes, which may overlap:

- those based upon an *a priori* error estimate acting directly on the equations of the problem (see e.g. [4]);
- those based on an *a posteriori* error estimate where the computed solution $u_h^n(\vec{x})$ is used to define the error (see e.g. [5], [7], [8], [9], [22]) (the index h denotes here a discretised solution);
- those which evaluate a combination of the derivatives of the computed variables (see e.g. [10], [31], [37]).

This latter function may be combined with the first two criteria. It is in fact the only possible way for complex systems, as the first two methods are only exact for model linear elliptic/parabolic equations ([21]). The two first ways may also imply an expensive sub-algorithm resolution of a non-symmetric problem at each intermediate time-step to determine the error on the spatial part of the P.D.E. operator, which may heavily penalise the cost

of the calculations.

The criteria we develop here are based on these lines too, but where the finite element estimations coming from the original system of equations are exploited, ponderated by the relevant physical parameters.

As the error estimate can also give disparate values, it is necessary to perform some additional smoothing in order to get a sufficiently regular mesh. Such regularisation is required by the F.E. solver for accuracy and stability. We shall extend these ideas in the sequel.

1.3 Finite element error estimators

Let us recall some basic concepts on error estimates and adaptation criteria for finite-element triangulations. Throughout the sequel we are concerned with a P_1-Galerkin finite-element discretisation, (the general P_l context will not be detailed here).

Let us define the finite-element spaces V_h as discrete subspaces of the functional space $H^1(\Omega)$, made of piecewise polynomial functions defined on a triangulation $\mathcal{T}_h = \{T_k\}$ of the bounded domain $\Omega \subset \mathbb{R}^2$. When constructing these V_h spaces, certain conditions must be fulfilled in order to preserve the compatibility of the approximation with the underlying mathematical framework.

For a conforming P_1 finite element approximation,

$$V_h \subset H^1(\Omega), V_h \subset C^0(\overline{\Omega}), \tag{1.1}$$

$$V_h = \left\{ v \in C^0(\overline{\Omega}) \;/\; \forall T_k \in \mathcal{T}_h, v_h\big|_{T_k} \in P_1(T_k) \right\}, \tag{1.2}$$

where $P_1(T)$ is the space of polynomials from Ω into $\mathbb{R}$, of degree less than or equal to 1 with respect to the variables $(x_1, \ldots x_d) \in \mathbb{R}^d$.

When generating triangulations, and thus when adapting them, for example by local refinement, we have to respect some rules of *admissibility–conformality* of the mesh and obtain reasonable regularity of the resulting elements. These properties of the mesh lead to a *regular* family of triangulations $\{\mathcal{T}_h\}_h$ and they are in particular necessary for a good approximation of parabolic or elliptic equations.

In order to achieve this goal, the following fundamental hypotheses should be fulfilled:

(H1) $\left\{\mathcal{T}_h\right\}_h$ is a *regular* family of triangulations if

(i) There exists constants σ and β such that, if we call
h_k the diameter of the triangle $T_k \in \mathcal{T}_h$, (for instance, the longest side of T_k, and
ρ_k the diameter of the circumscribed circle in T_k,
then $\forall T_k \in \bigcup_h \mathcal{T}_h$

$$\beta \leq \frac{h_k}{\rho_k} \leq \sigma \tag{1.3}$$

β is a measure of the smallest angle admissible.

(ii) There exists h_{max} such that $h_k \leq h_{max}$ $\forall T_k \in \bigcup_h \mathcal{T}_h$, and

$$h = \max_{T_k \in \mathcal{T}_h}(h_k) \longrightarrow 0 \tag{1.4}$$

since $\forall T_k \in \mathcal{T}_h$, $c_1 h_k^2 \leq \int_{T_k} dx$ where c_1 is a constant > 0.

(iii) The intersection of any two triangles T_j and T_k is empty, or is a vertex, or is an edge, or the triangle itself.

(H2) There is affine equivalence for $\left\{\mathcal{T}_h\right\}_h$, i.e. there exists an invertible affine mapping $f : \mathbb{R}^d \rightarrow \mathbb{R}^d$ such that

$$T_l = f(T_k) \tag{1.5}$$

$$a_i^l = f(a_i^k) \tag{1.6}$$

where $a_i^l, i = 1, 2, 3$, denotes the three nodes errors of the triangle T_l.

(H3) Let $u \in V \subset H^{\alpha+1}(T_k)$ be a solution of a variational problem in $H^{\tilde{\alpha}+1}$. Let us define $\pi_1 u$ the P_1-interpolating function of u in in the triangle T_k. Then for any integer m with $0 \leq m \leq 2$, there exists a positive constant C, independent of T_k, u, and the approximation, such that:

$$|u - \pi_1 u|_{m,1} \leq C \frac{h_k^{2-m}}{(\sin \beta_k)^m} |u|_{2,1} \tag{1.7}$$

where β_k is the smallest angle of the element T_k,
$|.|_{m,1}$ is the H^1 semi-norm of order $m \leq 2$. (see e.g. [17]).

For P_1-interpolation, we have $\forall m, 0 \leq m \leq 2$

$$|u - \pi_1 u|_{m,\alpha} \leq C \frac{h_k^{2-m}}{(\sin \beta_k)^m} |u|_{2,\alpha} \tag{1.8}$$

One can see from this expression that, all other terms being equal, the interpolation is optimal when the triangle T_k is equilateral.

These considerations lead us to briefly discuss *a priori* finite-element error estimates. Consider the equation:

$$Au = f, \text{in } \Omega \tag{1.9}$$

for instance,the Poisson problem:

$$\begin{cases} \Delta u &= -f \quad \text{in } \Omega, \\ u &= \quad g \quad \text{on } \partial\Omega, \end{cases} \tag{1.10}$$

on a convex domain Ω, with $f \in L^2(\Omega)$. Then the variational formulation writes:

$$(A_h u_h, v_h) = (f_h, v_h), \forall v_h \in V_h, \tag{1.11}$$

and we have the following error estimate:

$$|u - u_h|_{H^1} < C |u - \pi_h u|_{H^1} \leq C' \left[\sum_{T_k} h_k |u|^2_{H^2(T_k)} \right]^{1/2}. \tag{1.12}$$

This suggests a way of "optimally" adjusting h_k as a function of $|u|_{H^2(T_k)}$, that is, by reducing h_k where $|u|_{H^2(T_k)}$ is big, and thus by controlling

$$\left\| h^\alpha \frac{\partial^2 u}{\partial X^2} \right\| \tag{1.13}$$

with $\alpha = 1, 2$, will optimise the rate of convergence. This is the principle of adaptive meshing - uniformly equidistribute the error enhancing the overall convergence.

However, this method is quickly expensive, as the error estimate are functions of all derivatives $\frac{\partial^2 u}{\partial x_i \partial x_j}$. Moreover, it can only be evaluated exactly for linear elliptic problems.

This leads to consider *a posteriori* error estimates, which are derived along the same lines as *a priori* estimates, but rely on the calculated solution. Such error estimates will give weaker conditions than the *a priori* ones, but prove to be more easily extended to parabolic and hyperbolic problems. Also, since they depend on the local residuals, they are simpler and cheaper to implement into existing computer codes. In [21], [22], such estimates read as follows for the Poisson equation:

$$\|u - u_h\|_0 \leq \alpha \left\|h^2 f_h\right\|_0 + \beta \left|D_{h,2}(u_h)\right|_0 \sim \left|h^2 R_h\right|_{L^2}, \tag{1.14}$$

where $R_h(u_h)$ represents the discrete residual $(Au_h - f_h)$, and $D_{h,2}$ denotes the discrete second derivative. We shall use this quantity throughout the sequel for the spatial part of our parabolic operator. It can be estimated as:

$$D_h^2 u_h\Big|_{T_k} = \max_{T_{k'} \in V(T_k)} \frac{\left|\vec{\nabla} u_h(G_{k'}) - \vec{\nabla} u_h(G_k)\right|}{|G_{k'} - G_k|} \tag{1.15}$$

where $V(T_k)$ is the set of neighbouring triangles to triangle T_k — i.e. having a common edge with T_k — and G_k is the centroid of T_k. We shall also use:

$$D_h^2 u_h\Big|_{T_k} = \max_{\text{edges} \in T_k} h_{\text{edge}} \left|\left[\frac{\partial u_h}{\partial n_{\text{edge}}}\right]\right| \tag{1.16}$$

where [.] denotes the jump of the gradient across the common edge. These evaluations correspond to discrete H^2 norms, hence we can use the estimate (1.14) as in [21], [22]. Some modifications of this estimate will be needed in our applications, since the source term f is a non-linear function of u corresponding to the finite reaction rate (see §2).

The above estimates, although derived for an elliptic problem, have sometimes been used as a guide to mesh adaptation for the solution of parabolic time-dependent problems. Then, they are just applied to the spatial "elliptic" operator. However, error estimates can be directly derived for time-dependent parabolic partial differential equations discretised using conformal finite elements, as we now briefly recall.

Let us consider the following nonlinear parabolic problem in

$$D = \Omega \times (0, T)$$

$$\begin{cases} u_t - \kappa \Delta u = f(x,t,u), \\ u(0,x) = u^0(x) \ \text{ in } \Omega, \\ u(x,t) = 0 \ \text{ for } x \in \Gamma = \partial\Omega, \end{cases} \tag{1.17}$$

with $\kappa > 0$. If f is C^1 in u, then it can be shown that the solution of (1.17) lies in $C^1\left[(0,T);C^2(\Omega)\right]$ (see e.g. [15], [16]).

Recently in [34], [35], Nochetto, Paolini and Verdi studied the dynamical mesh adaptation for a non-linear Stefan problem of the form (1.17) with $\kappa = \kappa(u)$, using similar arguments to what we will use below. However, we follow now the error estimate analysis of Ushijima for the heat equation [42].

Here are some of the key steps of the latter paper.

Let:

$$V = \left\{ v \in C^0\left(\overline{\Omega}\right) \ / \ v\Big|_\Gamma = 0 \right\}.$$

Let $\mathcal{T}_h$ be a regular triangulation, (see above) and define

$$V_h = \left\{ v_h \in V \ / \ \forall T \in \mathcal{T}_h, v_h\Big|_T \in P_1 \right\}.$$

The variational form of (1.17) with $f = f(t)$ can be written:

$$\begin{cases} \frac{d}{dt}(u(t),v) + a(u(t),v) &= (f(t),v), \\ u(t=0) &= u^0, \end{cases} \tag{1.18}$$

for all $0 < t \leq T$, with $u(t) \in V$ and $v \in V$.

Then, the standard mass-lumping discretisation of this problem reads (see e.g. [24]):

$$\frac{d}{dt}(S_h u_h(t), S_h v_h) + a(u_h(t), v_h) = (S_h f_h(t), S_h v_h), \tag{1.19}$$

with $u_h \in V_h$, $u_h(t=0) = u_h^0$; here S_h is the projection from V_h onto $\mathbb{R}^{dim(V_h)}$, such that $S_h v_h$ is the vector of the nodal values of v_h for all $v_h \in V_h$.

Then for $m \leq 2$, we have (see [18]):

$$\max_{0\le t\le T}\|u_h(t)-u(t)\|_{L^2(\Omega)} \le c\left\{\begin{array}{l} h^m \max_{0\le t\le T}\|u(t)\|_{H^m(\Omega)} \\ +h^m \max_{0\le t\le T}\left\|\frac{\partial u}{\partial t}\right\|_{H^m(\Omega)} \\ +h^m \max_{0\le t\le T}\|f(t)\|_{H^m(\Omega)} \\ +\|u_h^0-\Pi_h u^0\|_{L^2(\Omega)} \\ +\max_{0\le t\le T}\|f_h-f(t)\|_{L^2(\Omega)} \end{array}\right\}, \quad (1.20)$$

if $u(t)\in D(A^{1+m/2})$ and $\dfrac{\partial u}{\partial t}\in D(A^{m/2});(m\le 2)$.

Several of the terms in the right-hand side of (1.20) can be rewritten or bounded using Kato's stability conditions [28] or the maximum principle for linear parabolic operators. Let us give the broad lines of these bounds.

Using the Kato stability conditions for

$$V_h \subset H_c^1 \subset H^1 \subset L^2 \quad (1.21)$$

where H_c^1 denotes $\left\{u\in H^1(\Omega)\ /\ C_u\big|_{\partial D}=g\right\}$, we have

$$|\Pi_h u-u|_1 \le \varepsilon(h)\,|v|_{H_c^1} \quad (1.22)$$

and

$$\left\|e^{-tA_h}v_h\right\|_{H^1} \le C_0\,\|v_h\|_{H^1} \quad (1.23)$$

where A_h denotes the discretised operator associated to the bilinear form $a(.,.)$, [42].

Then the last term in equation (1.20) can be estimated by

$$\max_{0\le t\le T}\|f_h(t)-f(t)\|_{L^\infty} \le h\max_{0\le t\le T}|f_h(t)|_{H^{1,\infty}} \quad (1.24)$$

Thus for these finite element error estimations in the case of time dependent problems, first the spatial part of the P.D. operator $\left\{\frac{\partial}{\partial t}+A\right\}_h$ is considered. An optimal error estimation then includes the term

$$\sum_{e\in \text{edges}} h_e^{2m}\left|\left[\frac{\partial u_h}{\partial n_e}\right]\right|^2,\ u\in V_h \text{ and } m\le 2 \quad (1.25)$$

The new triangulation $\mathcal{T}_h$ should verify for all $u_h \in V_h$

$$\alpha_m \|h^m f\| + \beta_m D_h^m(u_h) \leq \delta, \; m = 1 \text{ or } 2 \qquad (1.26)$$

where δ is some tolerance level. Applying this to the time-dependent problem using Kato's stability and the maximum principle for linear parabolic P.D.E's [25], we obtain estimations of the form:

$$\begin{aligned} \|u(t) - u_h(t)\| \leq \quad & c_1 \left\|h^2 f\right\|_{(0,t)\times\Omega} \\ & + c_2 \int_{(0,t)\times\Omega} \|f\| \, dt \\ & + \text{the terms in (1.20)} \end{aligned}$$

At each intermediate remeshing step, the new triangulation $\mathcal{T}_h$ must verify regularity and conformity in order to carry out the calculation on the new mesh.

1.4 Local and Global error estimators

The above error estimators, for elliptic and parabolic problems, have been used by several authors. Babuška, Rheinbolt and Zienkiewicz ([4, 5]) applied widely *a priori* estimates to elliptic and parabolic linear problems, considering in the latter case the elliptic spatial operator for the spatial adaptation of the discretisation. However Bank, Eriksson, Rivara ([9, 20, 40]) preferred *a posteriori* estimates.

In the framework of dynamical adaptation procedures for unsteady phenomena, we can also quote the works of Book, Boris, Eriksson and Johnson, Löhner, Morgan, Nochetto and Paolini, Peraire, Verdi and Vahdati ([21, 31, 30, 34, 36]). In any case, the adaptation criterion choice starts with the study of the spatial part of the partial derivative operators, even for hyperbolic problems, such as the Euler equations. The former authors use the elliptic techniques sketched above in order to obtain their local estimator. The latter ones base their local *a posteriori* estimators upon linear parabolic problems.

For the sake of completeness, let us mention the possible use of physical criteria. In this type of methods, the mesh is refined where the gradients of certain quantities are large [1, 2, 3, 37]. The strategy used in any such case

is similar: one defines an adequate local error estimate per element $\eta(T_k)$, and proper *tolerance levels*:

$$\max_{T_k} \frac{\eta(T_k)}{\tilde{\eta}(T_k)} = \delta \tag{1.27}$$

Here, $\tilde{\eta}(T_k)$ can for instance concern the neighbours of T_k, or the estimate on the "father" triangle of T_k, i.e. a triangle of the previous unrefined level. If the ratio $\frac{\eta(T_k)}{\tilde{\eta}(T_k)} > \delta$, then T_k is to be refined.

For instance, in [31], the authors use an estimate of the H^2 semi-norm, and then balance this value with the absolute value of the first derivative, in such a way that it filters out secondary noise and let every discontinuity be of the same importance, thus detecting secondary weak shocks as well as straight shocks. In [36], a P_1 approximation and a standard FCT algorithm is used, and the node-wise estimate:

$$E_i^2[(j)] = \frac{\sum_{k,l} \left(\int \varphi_i^k \varphi_j^l d\Omega \cdot U_j \right)^2}{\sum_{k,l} \left(\int_\Omega \left| \varphi_k^l \right| \left\{ \varphi_j^l U_j + \theta \left| \varphi_j^l \right| |U_j| \right\} d\Omega \right)} \tag{1.28}$$

is introduced, where φ_i is the P_1 basis function for node i, U_j represents the density at node j and θ is an adjustable parameter "to detect noise".

The choice of the density for the variable U allows good detection of shocks and secondary shocks in transient problems. Indeed, the jump of the gradient of the density is sharp across shocks, and an estimate of its second derivative therefore adequately detects the location of this jump, rather than the mathematical foundation of an *a priori* error estimation. This choice is also related with the fact that the FCT scheme is essentially a characteristic method for the continuity equation, i.e. that the density is the key variable for this scheme.

The close relationship between the scheme employed, the artificial dissipation or numerical viscosity within, and the efficiency of the mesh adaptation criterion is present in all mesh adaptation techniques.

To sum up this long introduction on some finite-element adaptive mesh techniques, let us recall that a survey of similar methods has been written by

Johnson [27] during completion of this work. In particular, a detailed error estimate analysis for parabolic problems is given in [27] using discontinuous Galerkin space-time finite-element discretisations, and streamline upwind space-time finite elements for hyperbolic problems are described.

We can also mention another totally different type of dynamical mesh adaptation which does not involve mesh refinement. Instead it consists in *moving* the nodes of the triangulation to follow the phenomena. Such methods can be based upon an optimisation problem related to the equilibrium of the mesh submitted to fictitious springs between the nodes with some given stiffness. This leads to costly resolution by iterative meshes, but gives very satisfactory results for shock capturing in steady-state solution calculations ([26]). However the quality of the triangulations can considerably deteriorate and the use of these techniques for fast reaction rate problems would not be optimal.

2 Reaction-diffusion model

The system of equations describing the low Mach number combustion of a premixed laminar flame can be given by the following simplified set of equations, known as the *thermo-diffusive model*. This is a simplified reaction-diffusion system, which retains the main features of low Mach number premixed flame propagation (see e.g. [12, 13]). Let us derive briefly this model from the following simplified set of reaction-diffusion equations:

- continuity equation

$$\frac{\partial \rho}{\partial t} + div(\rho \vec{v}) = 0 \tag{2.1}$$

- momentum equation

$$\frac{\partial \rho \vec{v}}{\partial t} + div(\rho \vec{v} \cdot \vec{v}^t)^t + div(p) = 0 \tag{2.2}$$

- energy equation

$$\frac{\partial \rho \vec{e}}{\partial t} + div((\rho e + p)\vec{v}) = D_T \Delta T + Q\Omega(T, Y) \tag{2.3}$$

- mass fraction conservation

$$\frac{\partial \rho Y}{\partial t} + div(\rho Y \vec{v}) = D_Y \Delta Y - \alpha \Omega(T, Y) \tag{2.4}$$

- reaction rate

$$\Omega(Y, T) = K Y \exp\left(-\frac{\mathcal{E}_a}{T}\right) \tag{2.5}$$

where $(\rho, \vec{v}, p, e)$ represent the hydrodynamical variables of mass density, velocity, pressure, and total energy of the mixture repectively. Y represents the mass fraction of the reactant R, T denotes the normalised mixture temperature, D_Y and D_T are the normalised diffusion coefficients, coming from respectively Fick 's and Fourier's law. Ω is the normalised reaction rate, Q represents the heat produced by the reaction, and $\mathcal{E}_a$ the adimensionalised activation energy .These are all standard parameters defining the combustion and can be given in explicit form from asymtotic analysis. K is the Arrhenius constant. Since we consider a premixed situation, the above equations may be closed by the state equation:

$$m_{\mathcal{R}} p = \rho R T \tag{2.6}$$

where $m_{\mathcal{R}}$ denotes the mass of the consumed reactant R.

Assuming low Mach number, the convective part may be simplified further, via an *isobaric* hypothesis. The above system becomes

$$\begin{cases} \frac{D}{\partial t} T &= D_T \Delta T + Q\Omega + f(p, \frac{\partial p}{\partial t}) \\ \frac{D}{\partial t} Y &= D_Y \Delta Y - \alpha \Omega \end{cases} \tag{2.7}$$

where $\frac{D}{\partial t} = \frac{\partial}{\partial t} + \vec{v} \cdot \vec{\nabla}$.

A further simplification comes from decoupling the hydrodynamics part from the the reactive part within the numerical alogorithm employed. The Euler equations (above) produce a solution $U = (\rho, \rho\vec{v}, \rho e, \rho Y)$, which is updated from the reactive part via the state equatoin. We may thus extract the following simplified system for a flame propagating in a two-component mixture, with the single one-step reaction $\mathcal{R} \rightarrow \mathcal{P}$:

$$\begin{cases} \frac{\partial}{\partial t} T &= D_T \Delta T + \Omega \\ \frac{\partial}{\partial t} Y &= D_Y \Delta Y - \Omega \end{cases} \tag{2.8}$$

Together with appropriate initial and boundary conditions which we write precisely below, this system is a stiff parabolic system with disparate time and length scales, which must be appropriately resolved in order to calculate an accurate solution. We refer to e.g. [11, 12, 13] for more details.

The typical spatial structure of the flame is given by the Figure 2.1, below where the variables T, Y, and Ω are represented schematically. The flame thickness L_f is extremely small within the reaction zone, requiring a high degree of mesh refinement to obtain a correct evaluation of flame speed, for instance. However, a coarse mesh would be sufficient within the regions of mixture and burnt gas zones where the variables T, Y, and Ω are approximately constant.

The whole problem is transient, thus the time-dependent properties of each variable couples with the spatial discretisation requirements for accuracy. During the initial phase, the gases are heated by conduction, in the preheat zone, then at ignition point the reaction zone begins. The flame front is propagating from right to left, with speed $v_f \approx \frac{L_f}{T_f}$. This speed may also be calculated by asymptotic theory [43, 41], and is a useful parameter to analyse the precision of the numerical method described in more detail below.

3 Auto-adaptive finite element method for unsteady problems

The stiff coupled non-linear parabolic system describing the thermo-diffusive part of the flame propagation given in section 2, needs an efficient algorithm in time and in space to correctly calculate the characteristic transient phenomena. This is the basis of the auto-adaptive finite element method.

A fourth-order Runge-Kutta method is used to integrate the time-dependent model in time, and discretised in space by P_1-Galerkin finite elements, on a family of (time-dependent) triangulations

$$\left\{\mathcal{T}\right\} = \left\{\mathcal{T}_h^{\mathrm{kt}}\right\}_{h\in\mathcal{H}}^{\mathrm{kt}=1,\ \cdots,\ \mathrm{ktmax}}$$

kt denoting the time iteration count, $\mathcal{H}$ indexing the spatial discretisation, generated by the adaptive refinement procedure. The refinement decisions are based upon a local error estimate, which has to be carefully chosen in

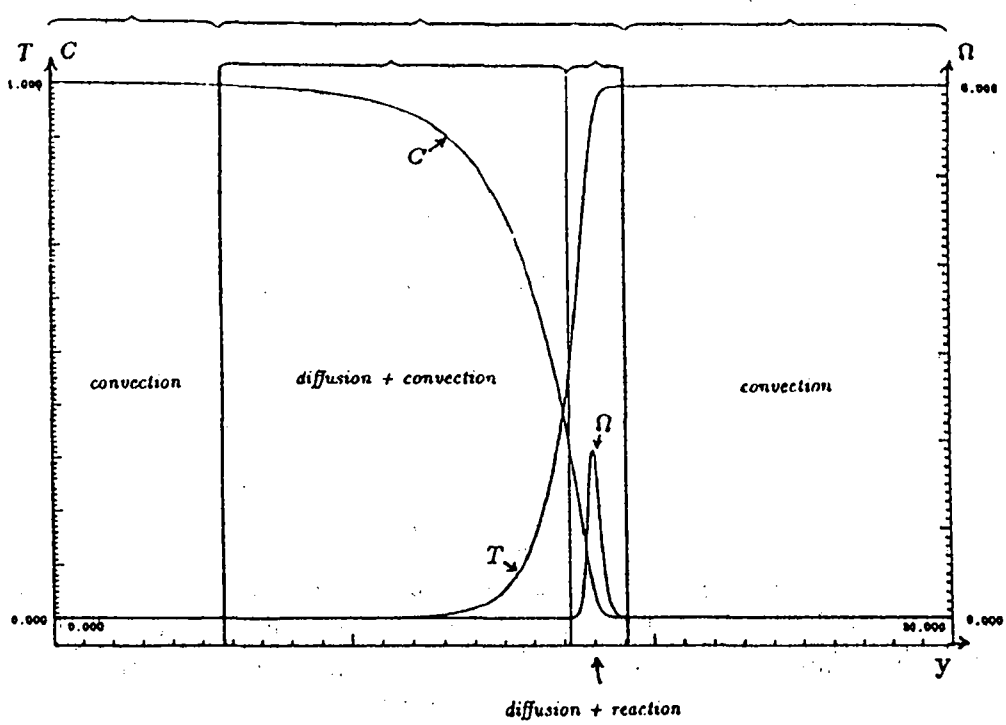

Figure 2.1: Structure of premixed flame

order to be as close as possible to the global error $\|u - U_h\|$, where u denotes the exact solution (T, Y) and U_h the discrete solution.

The updated solution u_h^n on $(\mathcal{T}_h^n)$ at time t^n is thus used to define a global estimation of the error. The global algorithm is a split (one step hydrodynamics)/(one step reactive part). This latter step is discretised by the P_1-Galerkin finite element approximation detailed in the next section above, and integrated in time by an explicit Euler method.

3.1 Discrete approximation

In practice, the system is solved with a convection term of given velocity $\vec{V}$, either taken to 0, i.e. system (3.1) then reduces to (2.8), or to the flame

speed, as proposed in [11, 12, 13]:

$$\begin{cases} \dfrac{\partial}{\partial t}T + \vec{V}\cdot\vec{\nabla}T &= D_T\Delta T + \Omega \\ \\ \dfrac{\partial}{\partial t}Y + \vec{V}\cdot\vec{\nabla}Y &= D_Y\Delta Y - \Omega \end{cases} \tag{3.1}$$

The boundary conditions associated with system (3.1) will be of the following simple form:

$$\begin{cases} T = T_u\ ,\ Y = Y_u \text{ on } \Gamma_{in} \\ \\ T = T_b\ ,\ Y = Y_b \text{ on } \Gamma_{out} \\ \\ \dfrac{\partial T}{\partial n} = 0\ ,\ \dfrac{\partial Y}{\partial n} = 0 \text{ on } \Gamma_{wall} \end{cases} \tag{3.2}$$

Here the boundary of the computational domain, Γ, is assumed to be divided into three parts representing respectively the inflow and outflow boundaries and a wall. Thus we have $\Gamma = \Gamma_{in} \cup \Gamma_{out} \cup \Gamma_{wall}$. The boundary values T_u and Y_u (respectively T_b and Y_b) denote the temperature and mass fraction of the unburnt gas at the inflow boundary (resp. of the burnt gas at the outflow boundary).

Let u denote the vector $(T, Y)^t$. Then if $t^n = n\Delta t$ denotes the time level of the interval $D \times [t^{n-1}, t^n] = D \times I_n$, we may reasonbly assume that [42, 28]:

$$\begin{cases} \|u(t^n)\|_{L^2(D)} \le C_1\|u(t^n - 1)\|_{L^2(D)} \\ \|u(t^n)\|_{J^2(D)} \le C_2(t)(1 + \Delta t)\|u(t^n - 1)\|_{L^2(D)} \\ \Omega \in C((0, t_n); L^2(D)) \end{cases} \tag{3.3}$$

¿From analysis of the thermo-diffusive system, we know that $Y \in [0, 1]$, and that T is positive but unbounded.

System (3.1) is simply discretised in space using the mass-lumped P1 finite-element approximation. We refer to [12, 13] for more details on the discretisation and on the evaluation of the time-step.

3.2 Discrete approximation

Let

$$\overrightarrow{u} = (T, Y)^t \tag{3.4}$$

The system can be written in detail as

$$\begin{cases} \dfrac{\partial u}{\partial t} &= \Lambda \displaystyle\sum_{i=1}^{2} \frac{\partial^2 u}{\partial x_i^2} + Q' \cdot \Omega(Y,T) \\ \Omega(Y,T) &= \kappa_0 \cdot Y \cdot \exp^{-\frac{\beta}{T}} \end{cases} \tag{3.5}$$

where Λ is the diagonal matrix of the normalised transport coefficients.

$$\Lambda = \begin{pmatrix} D_1 & \bigcirc \\ & \ddots \\ \bigcirc & D_2 \end{pmatrix} \text{ and } Q' = \begin{pmatrix} Q \\ -\alpha \end{pmatrix} \tag{3.6}$$

which is in fact a function of $(\overrightarrow{x}, t, u)$, and is taken to be locally constant at each fixed state in $(\overrightarrow{x}, t)$ (3.5) considered on a finite domain, $D \subset \mathbb{R}^2$, representing, for example, a combustion chamber — say, flame propagation from ignition — or modelising a semi-infinite cylinder — for studying relaxed winkled flame asymptotics.

Let $\mathcal{T}_h^n$ denote a triangulation of domain D at time $t = n\Delta t$, and let us define

$$\begin{aligned} V_h^n &= \left\{ v \in C^0(D) \;/\; v\big|_{T_k \in \mathcal{T}_h^n} \in P_1 \right\} \\ V_h^- &= \left\{ v \in V_h \;/\; v\big|_{\Gamma_{in}} = 0 \right\} \\ V_h^+ &= \left\{ v \in V_h \;/\; v\big|_{\Gamma_{out}} = 0 \right\} \end{aligned} \tag{3.7}$$

Then the variational formulation of (3.5) with approximate boundary conditions leads to the following discrete approximation.

$$(P_1)\begin{cases} \text{Find } u_h = \sum_{i\in I} u_i(t)\rho_i(x) \text{ such that} \\ \int_{D_h}\left(\sum_i \frac{du_i}{dt}\varphi_i\right)\varphi_j \;=\; -\int_{D_h}\Lambda\left(\sum_i u_i(t)\nabla\varphi_i\right)\nabla\varphi_j d\overrightarrow{x} \\ \qquad\qquad\qquad\qquad +\int_{D_h} Q'\Omega(u_h)\varphi_j d\overrightarrow{x} \\ \forall\varphi_j \in V_h^2,\ j\in I_0 = \left\{ii\in I \;/\; ii\notin I_{\text{in}}\cup I_{\text{out}}\cup I_{\text{wall}}\right\} \end{cases} \tag{3.8}$$

D_h denotes the discretised domain D, by the current triangulation $\mathcal{T}_h^n$.

The boundary terms are imposed within the variational formulation in the usual way, by considering the problem

$$(P_2)\begin{cases} \text{Find } u_h \in V_h^2 \text{ such that} \\ \int_{D_h} M\left(\sum_i \frac{du_i}{dt}\right) \;=\; -\int_{\mathcal{T}_h^n}\Lambda\left(\sum_i u_i\nabla\varphi_i\right)\nabla\varphi_j d\overrightarrow{x} \\ \qquad\qquad\qquad\qquad +\int_{\Gamma_{\text{wall}}}\Lambda\frac{\partial u}{\partial n} d\overrightarrow{x} \\ \qquad\qquad\qquad\qquad +\int_{\mathcal{T}_h^n} Q'\Omega(u_h)\varphi_j d\overrightarrow{x} \\ \forall\varphi_j \in V_h^2\cap V_h^-\cap V_h^+ \end{cases} \tag{3.9}$$

M denotes the diagonalising mass matrix given by a suitable choice of scalar product,[23].

$$\int_k(\varphi_i,\varphi_j)d\sigma = \text{Area}(C_i)\int_{C_i}\varphi_i\varphi_i d\sigma \tag{3.10}$$

C_i denotes the cell centered on node i, constructed by joining the gravity centres of each triangle connected to i.

Other discretisations using disparate approximation spaces with upwinding test functions $\{\varphi_h \in W_h \neq V_h\}$, or discontinuous Galerkin approximations can also be used [27].

Time integration is performed by explicit 4^{th} order Runge-Kutta integration to enlarge the stability domain of straight forward explicit Euler integration, as mentionned above.

For each time step $t^n = n\Delta t$

Let $u^{(0)} = u^{(n)}$

For $k = 1, \cdots 4$ do

$$u^{(k)} = u^{(k-1)} - \alpha_k \Delta t^n \left(\frac{du^{(k-1)}}{dt}\right)$$

then $u^{n+1} = u^{(4)}$

Local time stepping is employed. Since we are using here a standard Galerkin approximation, and ignoring dissipative effects -- coming from the hydrodynamic coupling with the transport coefficients — then we may take the optimal time step to be:

$$\Delta t^n = \min(\Delta t_d^n,\ \Delta t_r^n) \tag{3.11}$$

where Δt_d corresponds to the optimal time step for the diffusive part

$$\frac{\partial u}{\partial t} = \Lambda \Delta u \tag{3.12}$$

so

$$\begin{aligned} \Delta t_d^n &\leq \frac{\min_{k \in \mathcal{T}_h^n} (h_k^n)^2}{2\max(D_1,\ D_2)} \\ &\leq \frac{\sqrt{2}}{2} \min_{k \in \mathcal{T}_h^n} (h_k^n)^2 \cdot \min(D_1, -D_2) \end{aligned} \tag{3.13}$$

with h_k^n denoting the smallest height of triangle $T_k \in \mathcal{T}_h^n$;
and Δt_r comes from the reaction term and corresponds typically to the discretisation of the decay time t_e of the consumed Y to e^{-1} of its original value:

$$\begin{aligned} \frac{dY}{dt} &\sim \mathcal{K}_0 Y \exp\left(-\frac{\mathcal{E}_0}{T}\right) \\ t_e &= \left\{-\mathcal{K} \exp\left(-\frac{\mathcal{E}_0}{T}\right)\right\}^{-1} \end{aligned} \tag{3.14}$$

So

$$\begin{aligned} \Delta t_r^n &< \left[\mathcal{K}_0 \max_{i \in I} \exp\left(-\frac{\mathcal{E}_0}{T}\right)\right]^{-1} \\ &< \frac{1}{\mathcal{K}_0 \exp\left(-\frac{\mathcal{E}_0}{T_b}\right)} \end{aligned} \tag{3.15}$$

where T_b represents the asymptotic burnt up gas temperature.

Grouping together these considerations, the discrete problem now reads

$$\left\{\begin{array}{l} \text{Find } u^n(t) = \sum_{i\in I} u_i^n(t)\varphi_i(\overrightarrow{x}) \in C^0([0,T], V_h^2) \text{ such that} \\ \frac{u^{n+1}-u^n}{\Delta t_h}\int_{T_h^n} M d\overrightarrow{x} = - \int_{\mathcal{D}_h \equiv \mathcal{T}_h^n} \Lambda\left(\sum_{i\in I} u_i \nabla\varphi_j\right)\nabla\varphi_j d\overrightarrow{x} \\ \qquad\qquad + \int_{T_h^n} Q'\Omega(u_h)\varphi_j d\overrightarrow{x} \\ \forall\varphi_j \in V_h^2 \cap V_h^- \cap V_h^+ \end{array}\right. \tag{3.16}$$

3.3 Error criteria

Let us now come to the question of defining the criterion on which the refinement and unrefinement decisions will be based for the adaptive solution of the convection-reaction-diffusion system (3.1)-(3.2).

Our basic criterion is inspired from the theoretical considerations on a posteriori error estimates, which we briefly recalled in the introduction, coupled with a parametric study.

From a direct analysis of the original reaction-diffusion system a global estimator of the error can be obtained, thus a *local* error estimator $\eta(k)$, which determines whether an element T_k should be subdivided can be defined. This localised error estimator comes out from the smoothness (and lack of smoothness) properties of the solution of the continuous problem (3.1), and is also related to the discretisation algorithm used. We shall see, for example, the effects of taking into account the truncation error or not. Although the complete system is considered, with the underlying coupling with the hydrodynamics via convection, the criterion is developed on the simplified thermal-diffusion part. A global criterion is always possible by taking the

$$\max_{T_k}(\eta_k(T,Y), |\nabla m_k|) \tag{3.17}$$

where m_k denotes the local mach number, and ∇m_k is its discretised gradient.

Let us consider the thermo-diffusive part as in (3.5):

$$\mathcal{A}u = \frac{\partial u}{\partial t} - \Lambda\Delta u = Q'\Omega(\overrightarrow{x}, t, u) \tag{3.18}$$

Then the global error estimations are

$$\|u(t) - U_n\|_{L^2} < \delta_1 \tag{3.19}$$

and

$$\|u(t_n) - u_h^n(t_n)\|_{L^2} < \delta_2 \tag{3.20}$$

where δ_1 and δ_2 depend on the different bounds of Ω, u, $\frac{\partial u}{\partial t}$ and Δu. They can be identified using analogous arguments to those of Ushijama [42] for the heat equation, since $Q'\Omega(\overrightarrow{x}, t, u) \in C([O,T]; L^2(\Omega))$ and even $\in C([O,T]; L^2(D))$.

Since $u = (T, Y)^t$ may be represented as

$$u = \underset{x \neq x'}{\text{sign}}(\mathcal{X}(x - x')) * u' \tag{3.21}$$

such that $\mathcal{X}(x) = H(x)$, we may assume that $u' \in C([O,T]; L^2(D)^2)$.

Then using the Kato stability conditions for

$$\frac{d\tilde{u}_h(t)}{dt} + A_h u_h(t) = \tilde{f}_h(t, \tilde{u}_h) \tag{3.22}$$

where $\tilde{u}_h$ represents the projection $\mathcal{S}u_h$ given by the mass-lumping projection on the subspaces

$$V_h^2 \cap V_h^- \cap V_h^+ \subset V_h^2 \subset H^1(\Omega) \subset L^2(\Omega) \tag{3.23}$$

we deduce for $t_n \in [0,T]$

$$\begin{aligned} &\max_{0 \leq t \leq T} \|u(t_n) - u_h(t_n)\|_{L^2(\Omega)} \leq \\ &\quad c\left\{h\left\{\max_{0 \leq t \leq T} |u(t)|_{H^1} + \left|\frac{\partial u}{\partial t}\right|_{H^1} + \max_{0 \leq t \leq T} h\,|f(t)|_{H^1}\right\}\right. \\ &+ \quad \left. c_2 \int_{t_{n-1}}^{t_n} \|f\|\,ds + \|\mathcal{A}_h(u_h) - \Pi_h \mathcal{A}_h u_h\|\right\} \end{aligned} \tag{3.24}$$

where Π_h denotes the standard P_1 interpolation, and $h = \max_{T_k} h_k$.
For each macro-element T_k, a local error estimation $\eta^n(T_k)$ can thus be defined, where

$$\eta^n(T_k) = \text{Area}(T_k)\zeta^n(T_k) \tag{3.25}$$

where $\zeta^n(T_k)$ is a local error estimate of $\|u_h^n - u^n\|_{T_k}$ of the form:

$$\zeta^n(T_k) = \frac{1}{T_b - T_u} \left\{ \begin{array}{ll} & \frac{1}{h^0} \left| D_T \left[\vec{\nabla} T^n \right]_{T_k} \right| \\ + & \left| \vec{V} \right| \left| \vec{\nabla} T^n \right|_{T_k} \Big| \\ + & \frac{1}{\text{Area}(T_k)} \int_{T_k} |\Omega^n| \end{array} \right\} + \frac{1}{Y_u - Y_b} \left\{ \begin{array}{ll} & \frac{1}{h^0} \left| D_Y \left[\vec{\nabla} Y^n \right]_{T_k} \right| \\ + & \left| \vec{V} \right| \left| \vec{\nabla} Y^n \right|_{T_k} \Big| \\ + & \frac{Q'}{\text{Area}(T_k)} \int_{T_k} |\Omega^n| \end{array} \right\} \tag{3.26}$$

Here, the first factors on each line are weight factors coming from the different scales of the variables T and Y: $Y \in [Y_b, Y_u]$ and $T \in [T_u, T_b]$. We have set $h^0 = \max_{T_k} h_k$, and the notation $\left[\vec{\nabla} T^n \right]_{T_k}$ stands for:

$$\left[\vec{\nabla} T^n \right]_{T_k} = \frac{1}{3} \sum_{\substack{T_{k'} \text{ neighbours of } T_k \\ l \in \text{edges of } T_k}} \left\{ \vec{\nabla} T^n \Big|_{T_k} \cdot \vec{n_l} - \vec{\nabla} T^n \Big|_{T_{k'}} \cdot \vec{n_l} \right\} \tag{3.27}$$

where $\vec{n_l}$ represents the outward normal as in Figure 3.1.

It is also possible to directly couple this criterion with the truncation error coming from the explicit time-stepping

$$\tau \sim \frac{\Delta t}{2} \left| \frac{\partial}{\partial t} (\rho u)^{n+1} - \frac{\partial}{\partial t} (\rho u)^n \right|, \; u = (T, Y)^t \tag{3.28}$$

then $\tilde{\eta}(T_k) = \eta(T_k) + \tau \Big|_{T_k}$.

However no great improvement in the results are noticed, although a stronger coupling between the different parts of the criterion $\eta(T_k)$ and the time evolution is present, (see results). We tried other different modifications of the above criterion: different weights for each term; adding other evaluations of the time derivative of the variables in order to take into account their temporal evolution in a better way... etc. The above criterion, where the weights of all terms (convective, diffusive and reactive) are chosen by mimicing the governing equations, appeared to be altogether adequate.

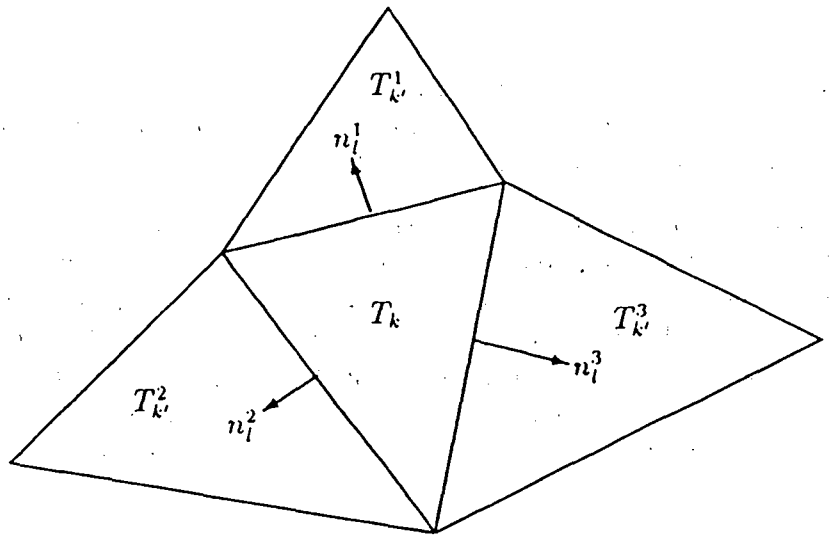

Figure 3.1: T_k neighbours and outward normal

The resulting criterion is extremely local, due to the stiffness of the problem, and the different scales of Y and T, there will thus be a tendency of mesh clustering of refined elements. Indeed the region where:

$$\nabla Y \cap \max \Omega \tag{3.29}$$

is not the same as

$$\nabla T \cap \max \Omega \tag{3.30}$$

In order to smooth out $\eta(T_k)$, and thus regularise the new triangulation $\mathcal{T}_h^n$, we proceed in two stages:

1. Within the solver's structure, the heat equation

$$\begin{cases} \frac{\partial G^n}{\partial t} = \Delta G^n & \text{in } D \\ \frac{\partial G^n}{\partial n} = 0 & \text{on } \Gamma_{in} \end{cases} \tag{3.31}$$

can be extracted and directly solved with little extra cost, as it is part of the governing equations of the system under consideration. We interpolate $\eta(T_k)$ onto the current mesh as initial condition, $\{\mathcal{T}_h^n\}$ to obtain

G^n. Then (3.31) is iterated up to $\|G\|_{H^2} \leq \epsilon$. By re-interpolation we obtain a smoother criterion which we will denote now by $C(T_k)$.

2. Normalisation of this $C(T_k)$ with respect to some reference value, (in order to normalise its value along the flame front, for example). We shall now discuss these possibilities in the next section.

We shall also present below the results of some computations where the adaptive refinement-unrefinement procedure is used for the solution of the unsteady Euler equations for perfect gas flow. In this case, the criterion used for the refinement decisions is mainly a heuristic one, such as the norm of the gradient of some quantity, like the density or the Mach number. Furthermore, for the computations of reactive flows, we mix the "flow criterion" used for the Euler equation with the "combustion criterion" (3.26) (see examples in §5 below).

3.4 Criterion averaging and normalising

As discussed above, the resulting criterion is to be smoothed out and/or averaged locally, then normalised with respect to some reference value before being able to make the refinement and unrefinement decisions.

We now describe and discuss four possibilities of normalisation.

3.4.1 Global maximum

The normalised criterion is then evaluated as:

$$C^n(T_k) = \frac{C(T_k)}{\max_{T_k} C(T_k)} \tag{3.32}$$

Then the normalised criterion satisfies $\max C^n = 1$, and we can use it in the simple following way:

> Let $(0 = b_0 < b_1 < \cdots < b_{lev+1} = 1)$ be a sequence of real numbers, where lev is the desired number of refinement levels. If the macro-element T_k is such that:
>
> $$b_i \leq C^n(T_k) < b_{i+1} \tag{3.33}$$
>
> then T_k is divided into 4^i subtriangles.

This method is simple, but supposes that there exists large zones of the computational domain D where $C(T_k) \sim 0$, and others where $C(T_k) \gg 0$, this ignoring intermediate values: the normalised criterion will not detect gradients or layers of secondary importance. On the opposite, if the criterion is almost constant, no matter it is big or small, we will refine almost everywhere at the uppermost level.

3.4.2 Local maximum

We take the maximum of the unnormalised criterion over T_k and its neighbours $T_{k'}$ as reference value:

$$C^n(T_k) = \frac{C(T_k)}{\max_{T_{k'} \Big/ T_{k'} \cap T_k \neq \emptyset} C(T_{k'})} \tag{3.34}$$

This method also has the advantage that the normalised criterion is known to take its values in the interval $[0, 1]$, which allows us to again make the decisions using (3.33). Now the secondary wave will be detected, but will be refined at the finest level as the main refined zones. This makes the resulting mesh very sensitive to small fluctuations in the unnormalised criterion values. And the same drawback as before again appears if the unnormalised criterion is almost constant.

These two preceding normalisations of the criterion make it particularly difficult to decide upon what thresholds b_i to use for the refinement decisions and to master the number of elements/nodes which the adaptation procedure creates. Moreover when the number of levels of refinement/derefinement changes then we have to redefine all the b_i's.

3.4.3 Mean value

Here, we evaluate the mean value $\overline{C}$ of the unnormalised criterion over the whole triangulation, and define the normalised criterion as:

$$C^n(T_k) = \text{Area}(T_k)\frac{C(T_k)}{\overline{C}} \tag{3.35}$$

This normalised criterion can be used as follows. Choosing a positive real number α, we say that the triangle T_k is divided into 4^i subtriangles if:

$$4^{i-1}(1+\alpha) < C^n(T_k) \leq 4^i(1+\alpha) \tag{3.36}$$

The interpretation of this is clear: a triangle is refined if it contains more than $1 + \alpha$ times the mean value $\overline{C}$ of the criterion.

This choice amounts to trying to equally distribute the criterion among all elements. In some sense, this choice minimises the CPU as it leads to refine almost nowhere if the variations of the unnormalised criterion are small. But this can also be a drawback if an accurate computation is expected.

3.4.4 Relative localised criterion

We can also choose to use as a local reference value the primitive variable F upon which the evaluation of the unnormalised criterion is based, for instance the temperature:

$$C^n(T_k) = \text{Area}(T_k)\frac{C(T_k)}{F(T_k)}$$

Thus, if the unnormalised criterion, C, is an approximation of the error (respectively of the evolution terms) then the normalised criterion, $C^n(T_k)$, is the relative error on (resp. the relative variation of) the variable F in the triangle T_k.

The thresholds which are used for the refinement decisions are then more meaningful: one can decide to refine an element if the relative change of the considered variable in this element is greater than, say, 5%. This choice of the reference value is very appropriate for ensuring a given accuracy or a good capturing of the phenomena under consideration. But, like the first two choices, it leads to a very difficult mastering of the number of elements created by the adaptation procedure.

4 ADAPT's algorithm

We give here a short introduction to the ADAPT algorithm. For more details and extensions developed, we refer to [14, 11, 32].

4.1 Description

The algorithm ADAPT, a dynamical local mesh refinement /unrefinement procedure, allows unsteady phenomena to be followed with precision during a simulation run. It is based on a certain number of basic algorithmic principles

taking into consideration the particuliarities of local mesh refinement for finite element type generated meshes.

The algorithm was first inspired by an adaptive multigrid algorithm. Which used different grid levels of non-constant subdivision to maintain smaller memory requirements. Indeed, each level was obtained as a local enrichment of a coarser level. Thus one could benefit from the convergence acceleration provided by use of a multigrid stategy within the numerical scheme of resolution.

Here we are concerned with *multi-levels* of refinement. The local refinement/unrefinement procedure is multi-level in time: at each significant eveolution of the simulation, the calculation mesh is modified by a multi-level local refinement or coarsening. For instance, in the cases presented here of triangular (2D) meshes, once a suitable regularised criterion (see §3) has been selected, the list of elements to be refined, their degree of refinement (division of triangles 4^N times, N being the refinement level), and those to be unrefined are established. So at each given remeshing step, the refinement procedure follows a multi-level hierarchical structure.

A suitable data-base structure must thus be defined in order to facilitate transfers of information, with dynamical memory allocation requirements provided by use of dynamical identifications for internal fagging (pointers). This data base structure is based upon a hierarchical data tree structure, where the successive filiations allow scans backwards and forwards within each data list.

Addition or suppression of data points or blocks corresponds to an internal extension of existing blocks within the data base. The global structure remains fixed. This allows for a minimal blank memory storage, otherwise prohibitive.

Other considerations must also be taken into account, coming from the actual solution algorithm on such meshes: at each remeshing phase, the output mesh should be renumbered, restructured for, for example, vectorisation considerations, and colouring graph techniques reapplied at each phase for gather/scatter operations. To facilitate a "black box" version of ADAPT, a kind of doubling of the data structure may be allowed (I/O) at the cost of greater memory usage.

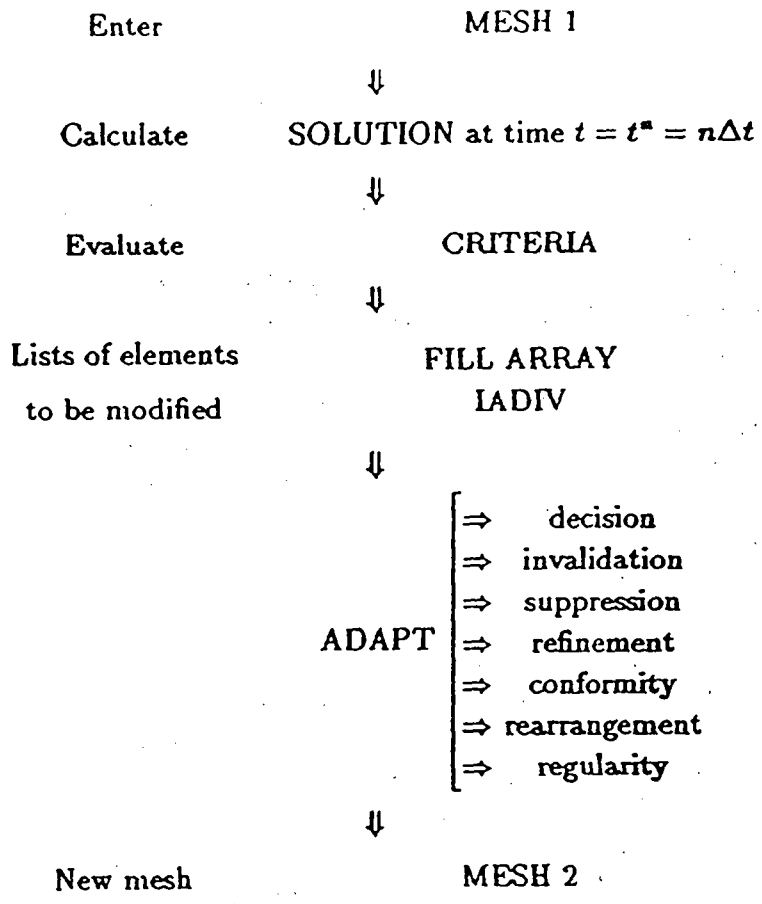

Figure 4.1: Programme Structure

4.2 Data Structure

The general procedure can be resumed by the organigram as in Figure 4.1.

Let us now go into more details. In the case of 2D triangular finite elements, a given triangle may be subdivided 4^N times. Then for conformity, neighbouring triangles may need to be divided into 2 or 3 subtriangles (the latter is always excluded as adamissible subdivision). This may lead to a lack of regularity, and a smoothing process is applied, i.e. neighbouring zones to a division into 4^2 are first dived into 4, then further out into 2. Starting from a basic *macro-mesh*, which remains unaltered within the whole procedure, we may cut up the data structure as indicated in the following Figure 4.2,

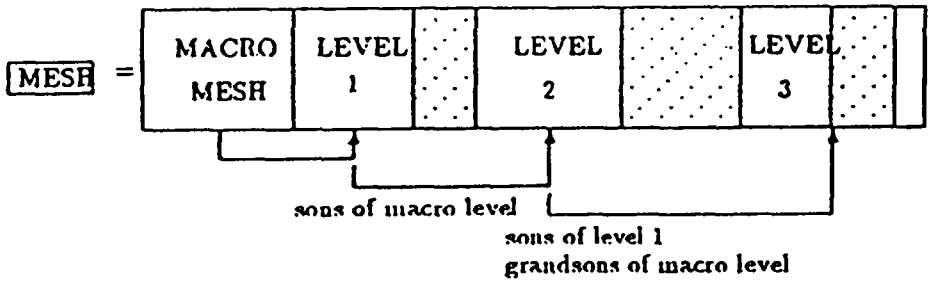

Figure 4.2: Mesh levels

The hashed block corresponds to dummy memory space. The invalidation phase corresponding to suppression and reintroduction of elements takes palce here. Globally, the data structure of such a given mesh is fixed by identifying arrays of pointers NE(2,LEVEL).

A given element K in the macro-mesh has an etiquette IFATHER, a value IADIV(K) determined by the criterion calculation phase, and a filiation decendence according to the Figure 4.3

IADIV(K) is the array defining the level of refinement per element, according to the criterion (see §3). Let us resume how it is determined in function of the refinement decision. This array indicates clearly the filiation:

- if IADIV(K) = 0 then K is not to be divided.
- if IADIV(K) = $N \succ 0$ then K is to be divided into 4 subtriangles and each of its sons has its IADIV set to $N-1$, i.e. each son will be divided into $4^N - 1$ subtriangles (and their IADIV(ISON) = $N-1$).

When a triangle K has to be invalidated and suppressed, its filiation must be also. Again, the array IADIV along with the identifiers NE(*,LEVEL), allow us to scan the list correctly.

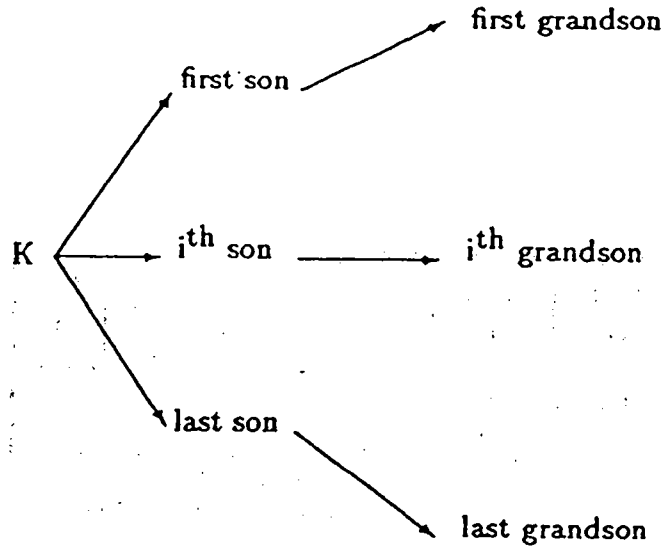

Figure 4.3: Filiation Tree

Division of a triangular element is undertaken by cutting each edge at its midpoint. An array ICUT(NEDGE) indicates which edges are to be cut. If ICUT is equal to -1, the edge number NEDGE has to be divided; if ICUT is equal to $NN \succ 0$, NN is the number of the node created at the midpoint; if ICUT is equal to 0, this edge is not cut. This array must be updated and reinitialised at each global step, after each global renumbering sweep.

4.3 Refinement Decision

As described in 3, after regularisation, a certain criterion $\tilde{\eta}(K)$ per element is adopted for the refinement/unrefinement decision, which is transmitted by the array IADIV(K).

Following §3, this procedure is implemented as in the figure 4.4, *levelmax* denotes the total number of levels of refinement per step.

define $\beta_{-1} = 0 < \beta_0 < \beta_1 < \cdots < \beta_{levelmax-1} < \beta_{levelmax} = 1$
For all elements K **in** Mesh 1 ($\mathcal{T}_h^n$) **Do**
  level := 0
  Until *level* = *levelmax* **Or** $\beta_{level-1} < \frac{\tilde{\eta}(K)}{\max_K \tilde{\eta}^n(K)} \leq \beta_{level}$ **Do**
    level := *level* + 1
  End Do
  IADIV(K) := *level*
End Do

Figure 4.4: decision loop

4.4 Refinement/unrefinement procedure

ADAPT may now be explicited by the organigram of Figure 4.5.

5 Results

Some of the results showed here were made with an old version of ADAPT that used to take as its input the decisions IADIV on the macro-elements and transmits them to the higher levels. This has changed now: the decisions are taken on the current refined mesh. This allows a finer resolution of refinement zones and results in a lower global overall number of nodes.

Firsly, different criteria are illustrated by standard shock tube simulations in order to see what each criterion was able to detect. As the goal was not so much the solutions's quality, but the detection ability of each criterion, the exact solutions are not illustrated . Then simplified combustion chamber calculations concerning the propagation of a flame front within a square chamber from an initial ignition zone on the upper side are simulated. Finally flame propagation within a semi-infinite duct are studied, in order to test the various criteria. For all calculations a standard P1 scheme for diffusive terms was employed.

5.1 Shock tubes with relative error

The criterion normalisation used in this section is the relative one (see §3.3 3.4.4). The normalised criterion for each element T_k is thus defined as:

$$C^n(T_k) = \text{Area}(T_k)\frac{C(T_k)}{F(T_k)}$$

where the functions $C(T_k)$ itself and $F(T_k)$ have to be chosen.

5.1.1 Adaptation on Mach gradients

The criterion used here is

$$\begin{aligned} C(T_k) &= \left\| \vec{\nabla}\mathcal{M}\text{a} \right\| \\ F(T_k) &= \max(\mathcal{M}\text{a}, \mathcal{M}\text{a}_{min}) \end{aligned}$$

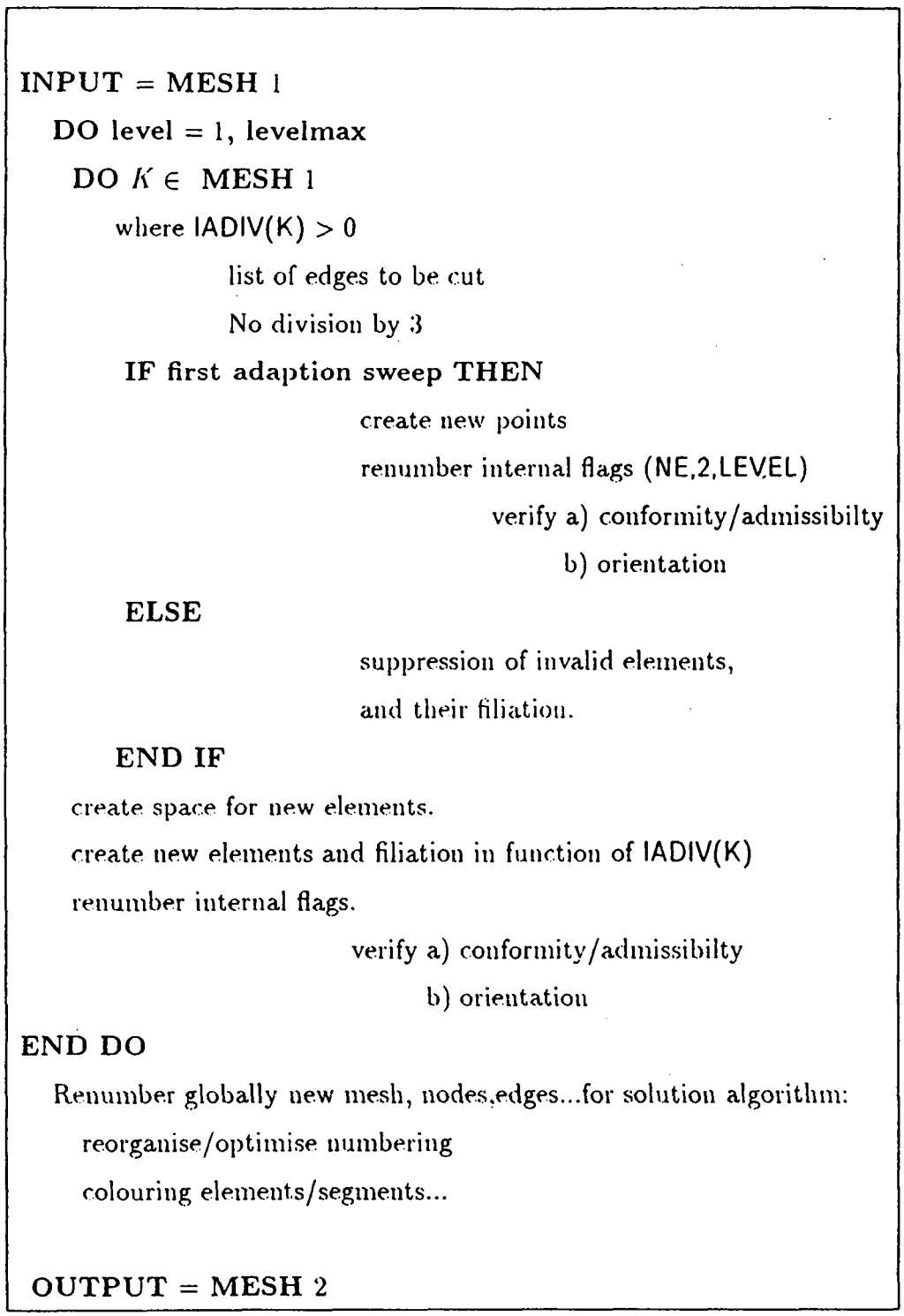

Figure 4.5: ADAPT Organigram

where $\mathcal{M}a$ is the Mach number and $\mathcal{M}a_{min}$ a threshold avoiding a division by zero.

We can see in figures 5.1 the contact discontinuity is almost missed with this criterion. This is due to the difference of height between the jump of the shock and the jump of the contact discontinuity. On the other hand, too much nodes are put in the expansion wave by that criterion.

5.1.2 Adaptation on temperature gradients

Here we use

$$\begin{aligned} C(T_k) &= \left\| \overrightarrow{\nabla} T \right\| \\ F(T_k) &= \max(T, T_{min}) \end{aligned}$$

where T is the temperature in the element and T_{min} a threshold. In that case the T_{min} value is not necessary the temperature being strictly positive.

As we expect with that criterion fewer nodes are created in the expansion wave and the contact discontinuity is captured better (see figures 5.2). That is why we choose this criterion for our calculations.

5.1.3 Adaptation following both gradients

A combination of the maximum of both the previous criteria is experimented here, (see figures 5.3). We can see that the $\mathcal{M}a$ relative criterion is much more important than the temperature one. In fact, this is due to the parts where the $\mathcal{M}a$ is near of 0. In the figures 5.3, the error tolerance level was of 2% that is when the normalised criterion is above that value the element is to be refined. In the figures 5.4, the level is 1.1%. We can clearly see the effect of the error tolerance level.

5.1.4 Shock tubes with error equidistribution

To illustrate another criterion normalisation and the effect of the order of the scheme, we use in this section the normalisation described in §3.3 3.4.3. So we define:

$$\overline{C} = \frac{1}{\mathrm{NT}} \int_{T_h^n} C(T_k)$$

and the normalised criterion can now write:

$$C^n(T_k) = \text{Area}(T_k)\frac{C(T_k)}{\overline{C}}$$

We also choose to use the maximum of both the criteria divided by their maximum as the criterion:

$$\begin{aligned} C_T(T_k) &= \left\| \vec{\nabla} T \big|_{T_k} \right\| \\ C_{\mathcal{M}a}(T_k) &= \left\| \vec{\nabla} \mathcal{M}a \big|_{T_k} \right\| \\ C(T_k) &= \max\left(\frac{C_T(T_k)}{\max_{T_i} C_T(T_i)}, \frac{C_{\mathcal{M}a}(T_k)}{\max_{T_i} C_{\mathcal{M}a}(T_i)} \right) \end{aligned}$$

Comparing figures 5.5 and 5.6, we see that the contact discontinuity is more precisely captured using a second order approximation, however the mesh is not altered significantly.

5.2 Combustion chamber

The criterion used here is

$$C(T_k) = \left\| \vec{\nabla} T \right\| \tag{5.1}$$

which is normalised with the "Mean value" method.

As said before in §3.3 3.4.3, this method only tries to equally distribute the criterion throuhout the domain. As can be seen in figures 5.7 to 5.9 the topmost level of refinement is not reached at all time steps of the calculation. The result is very satisfactory compared to the cost needed to obtain it.

5.3 FEM truncation error criterion

5.3.1 First version with ad-hoc parameters to be adjusted

The criterion tested now is the FEM truncation error. It should be the better one in theory. However there are two ad-hoc parameters that occur in the estimation, which are adjusted accordingly. Indeed, a considerable part of the phenomena (see figures 5.10 and 5.11)can be missed. Thus the choice of those parameters is crucial and cannot be free.

5.3.2 Second version with correct criterion

Here the same criterion is employed but where the parameters have been chosen directly from the governing equations. In that way their dimensions are correct and they give better results as shown in the figures 5.12 and 5.13. We can see now the phenomenon based criterion is simpler and more obvious than the FEM truncation error one.

5.4 Effects of regularisation of the criterion

We show here two different regularisations of the criterion. First, a very local method that only makes some mean value with the criterion in the element and in its neighbours. This method relies too much on the current topology of the mesh, that is: refined parts and boundaries. In figure 5.14, the mesh obviously shows inaccuracies in the boundaries.

The second method uses a Laplacian in order to regularise the criterion. It allows us to use an already computed Laplacian and regularises the criterion without moving the maxima (see figures 5.15).

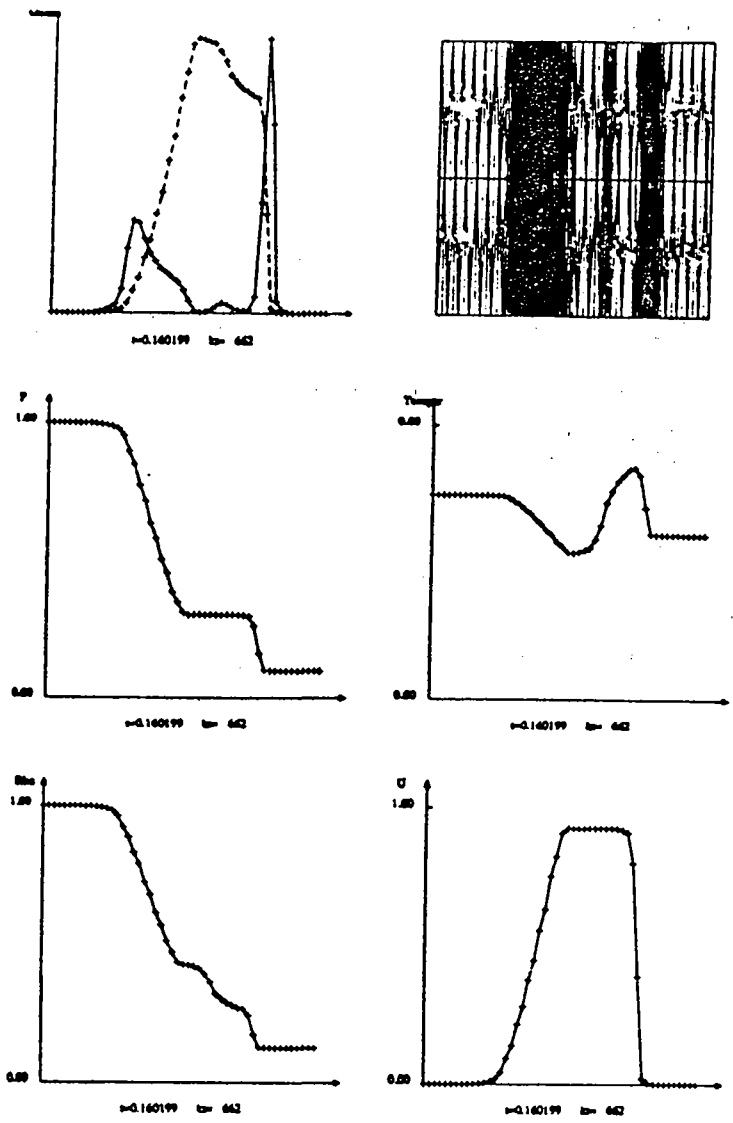

Figure 5.1: Shock tube with Mach criterion
From left to right and top to bottom, there are the Mach and criterion, the mesh, the pressure, the temperature, the density and the speed in the x direction.

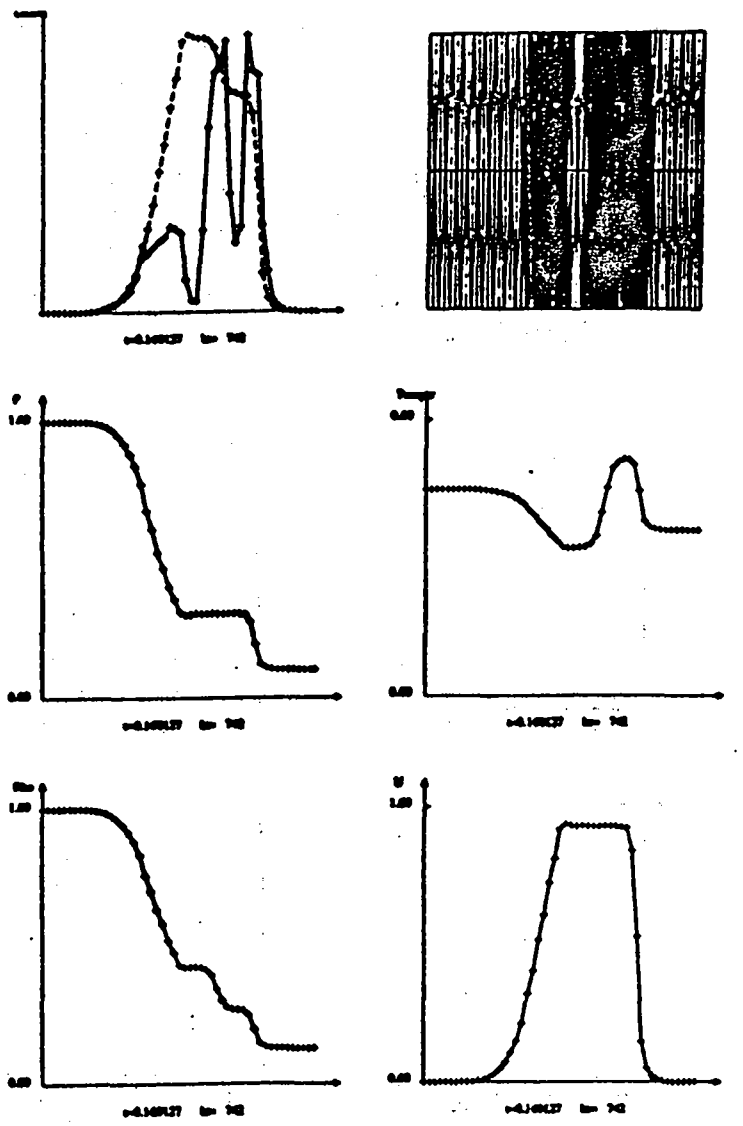

Figure 5.2: Shock tube with temperature criterion
See figure 5.1 for legend.

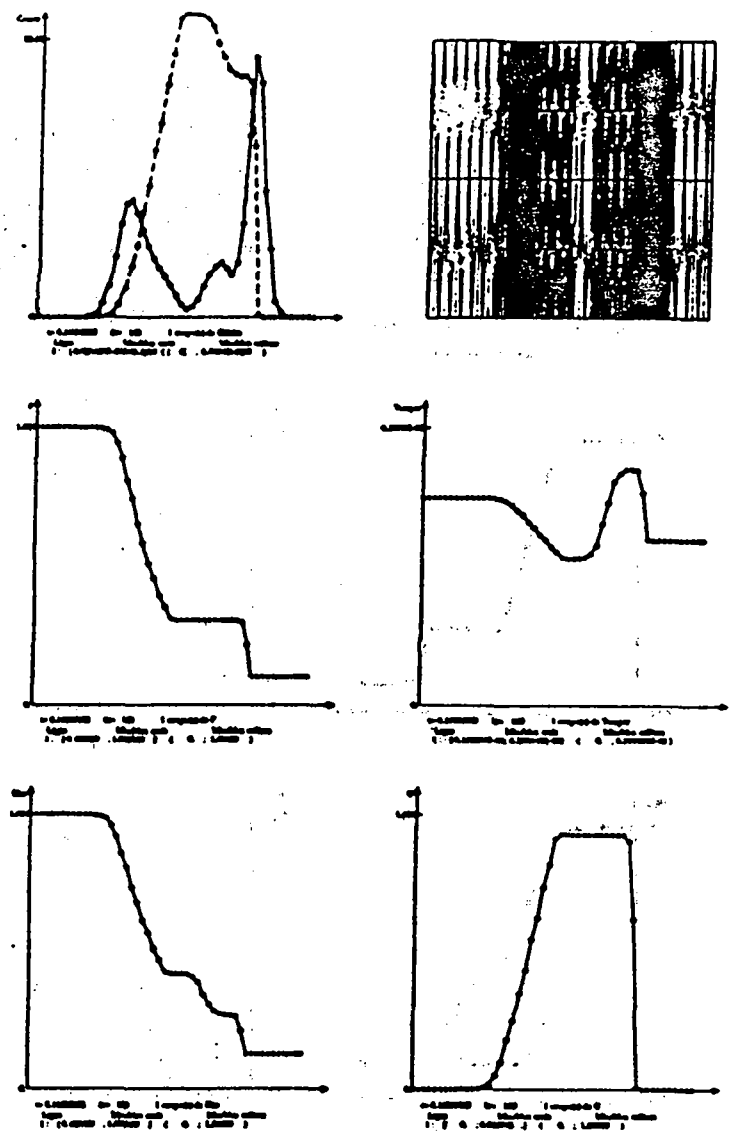

Figure 5.3: Shock tube with both criteria, 2% error
See figure 5.1 for legend.

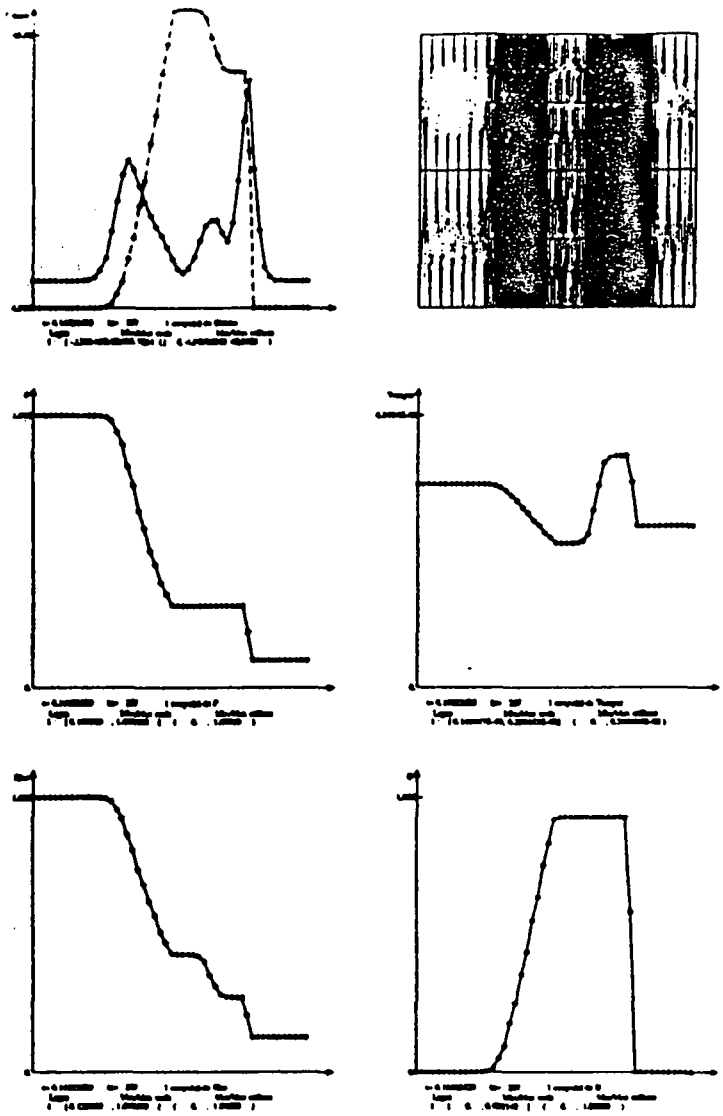

Figure 5.4: Shock tube with both criteria, 1.1% error
See figure 5.1 for legend.

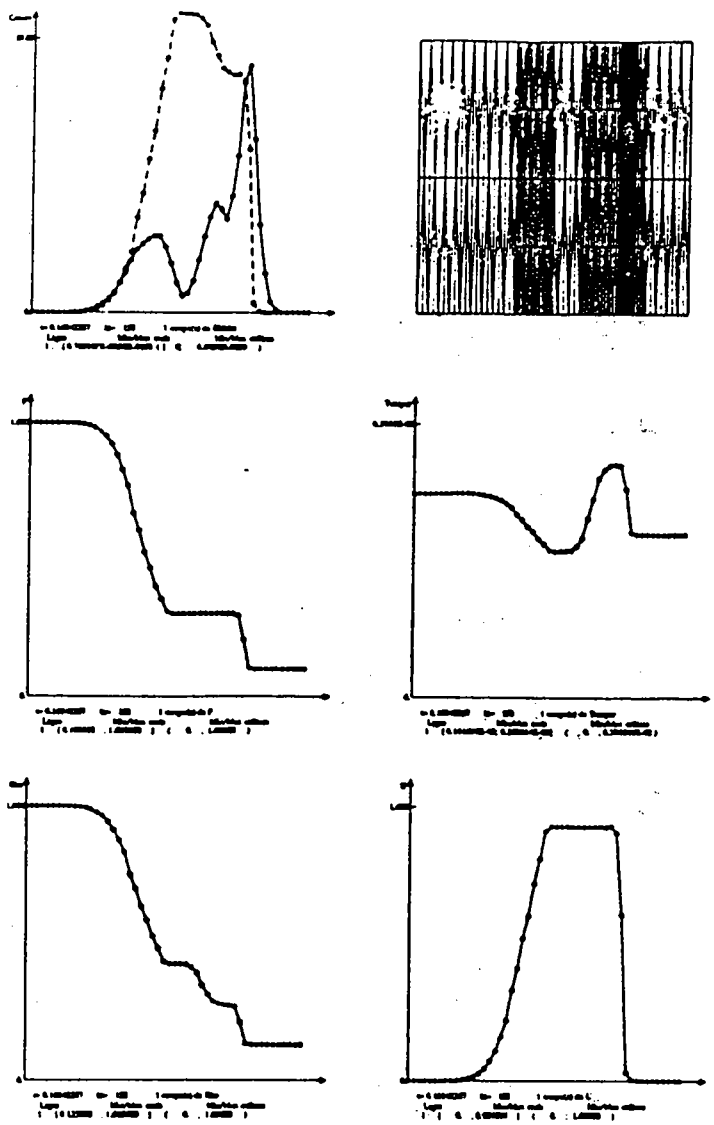

Figure 5.5: Shock tube with both criteria, equidistributed, order 1
See figure 5.1 for legend.

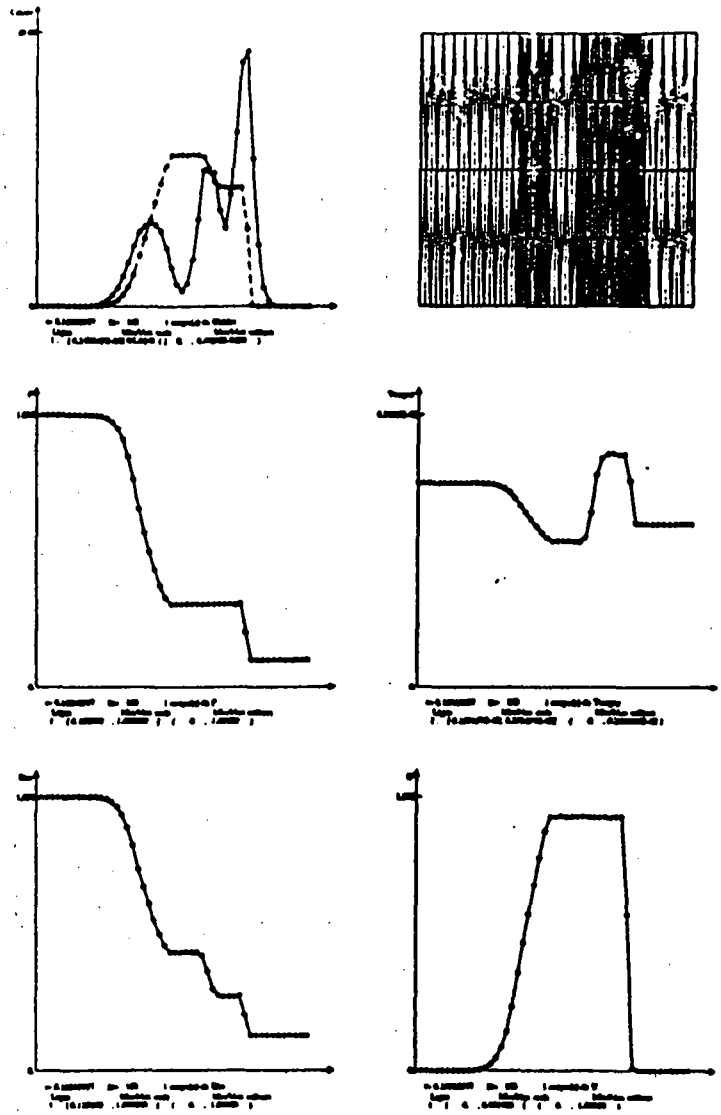

Figure 5.6: Shock tube with both criteria, equidistributed, order 2
See figure 5.1 for legend.

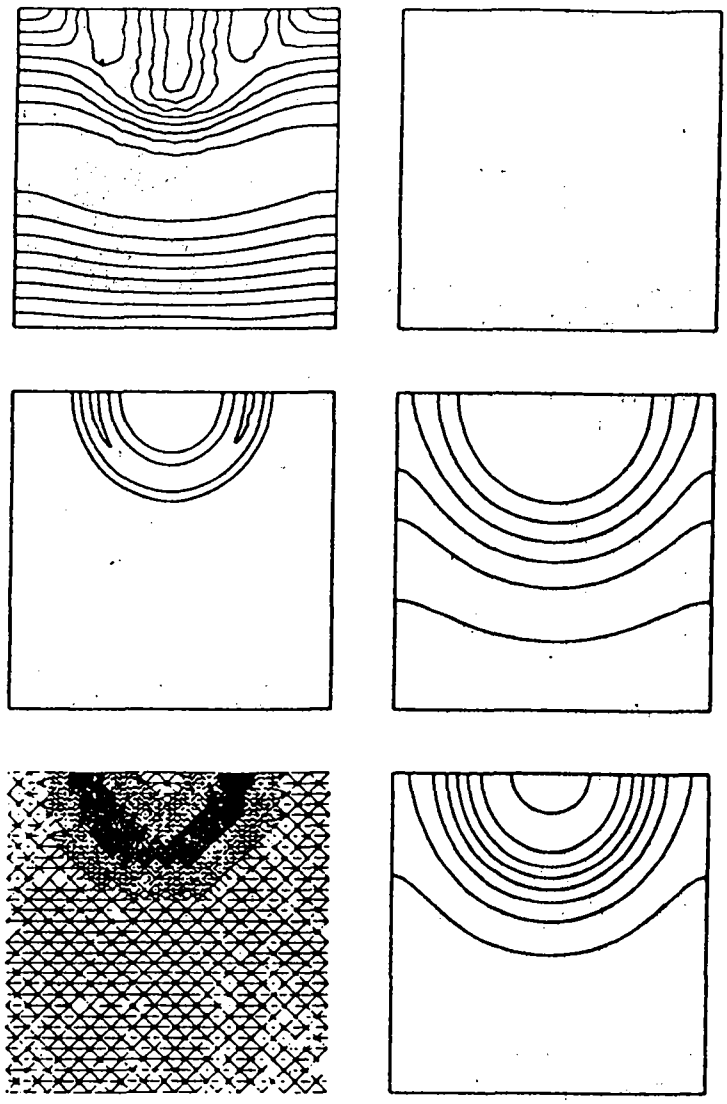

Figure 5.7: Combustion chamber with mean value normalisation $t = 3.5$ From left to right and top to bottom, there are the Mach, pressure, reaction rate, mass fraction contours, the mesh and the temperature contours.

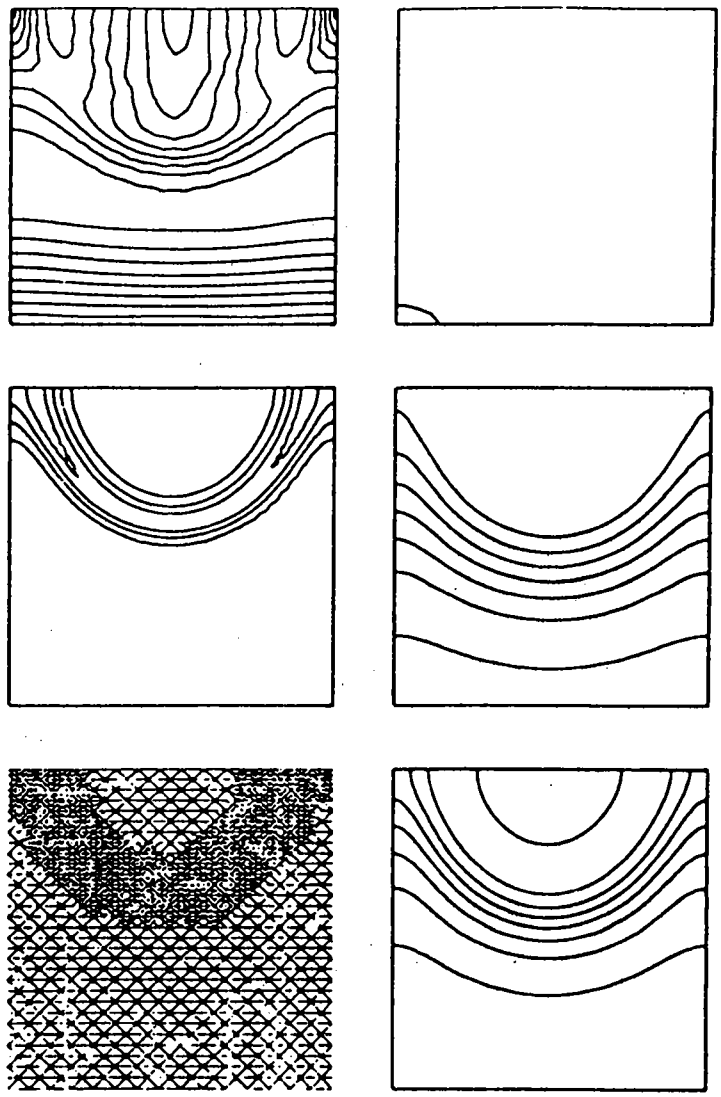

Figure 5.8: Combustion chamber with mean value normalisation $t = 4.5$
See figure 5.7 for legend.

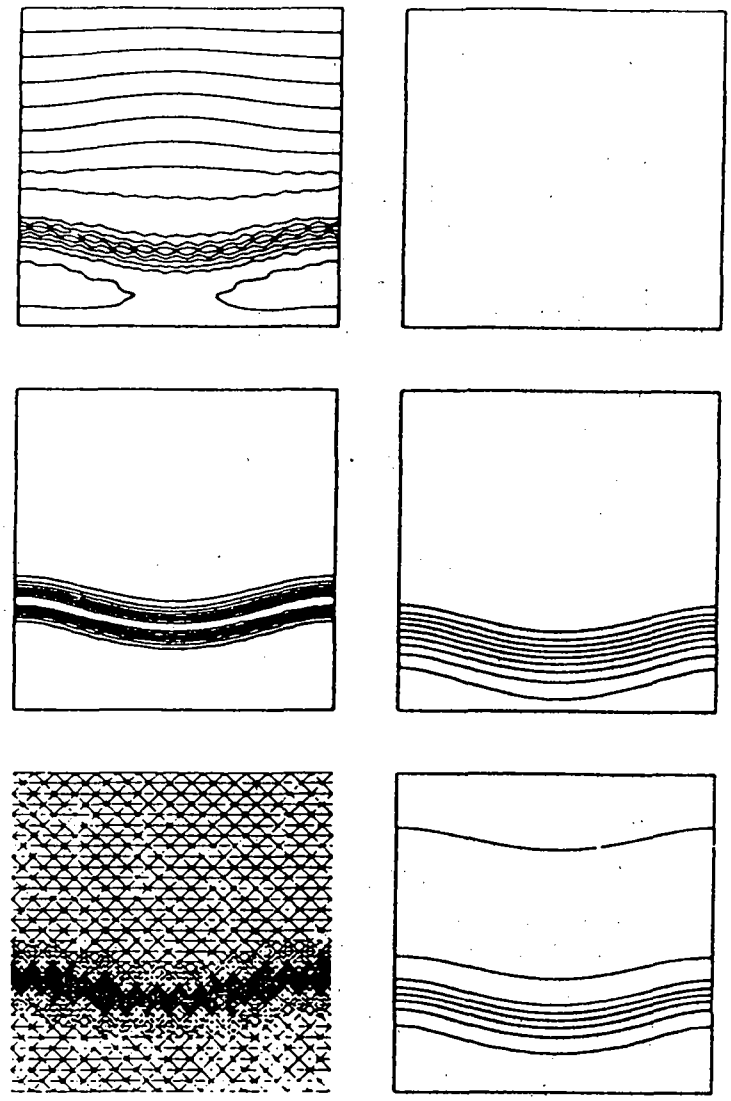

Figure 5.9: Combustion chamber with mean value normalisation $t = 7.0$
See figure 5.7 for legend.

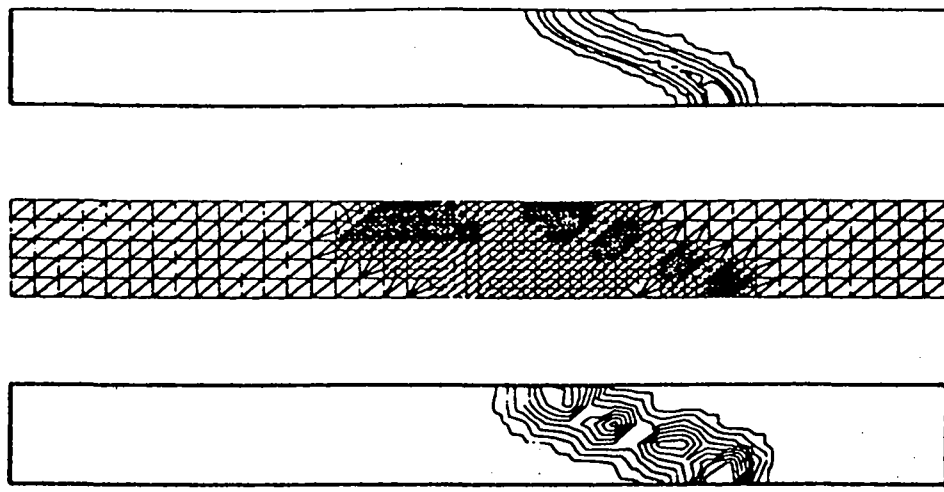

Figure 5.10: FEM error with random coefficients for a tube
From top to bottom, there are the temperature contours, the mesh and the reaction rate contours.

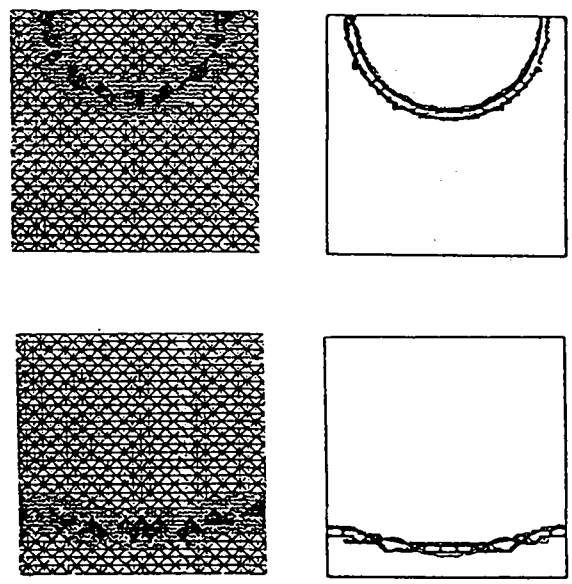

Figure 5.11: FEM error with random coefficients for a Combustion chamber
From left to right, there are the mesh and the reaction rate contours. We show here two different time steps.

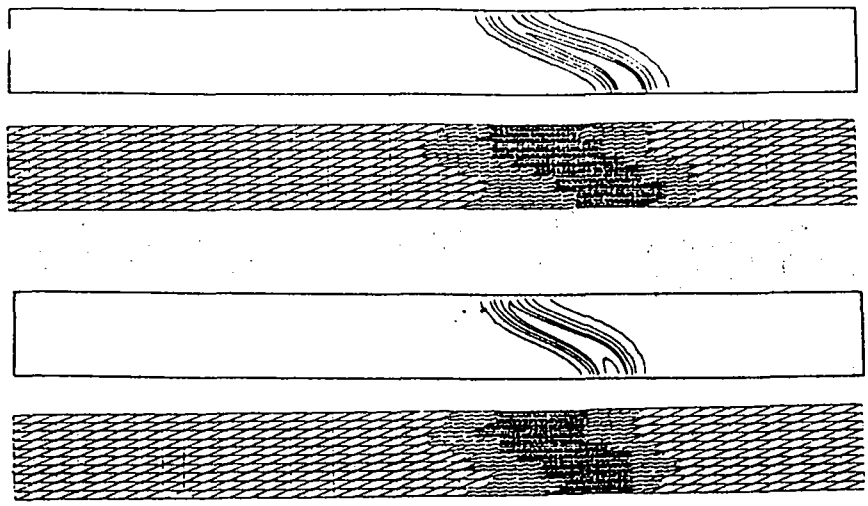

Figure 5.12: FEM error for a semi-infinite duct with coefficients coming directly from the equation system
From top to bottom, there are the reaction rate contours and the mesh.

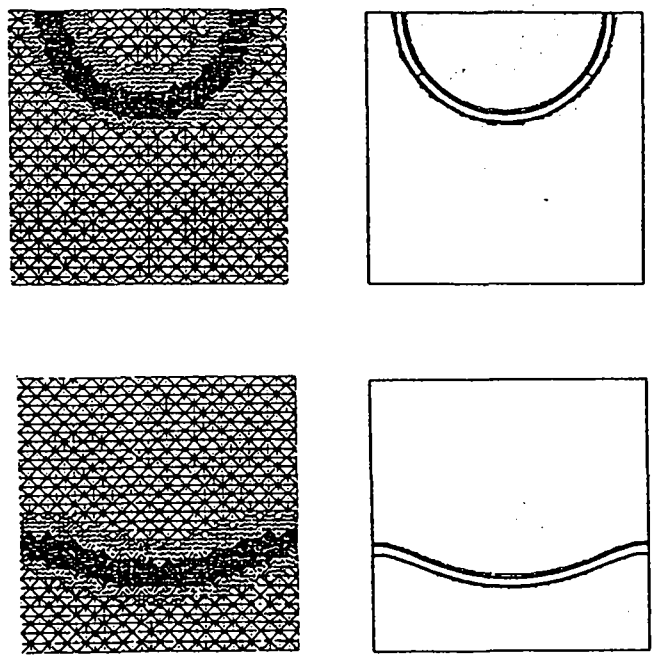

Figure 5.13: FEM error for the Combustion chamber experiment with coefficients coming directly from the equation system
From left to right, there are the mesh and the reaction rate contours. We show here two different time steps.

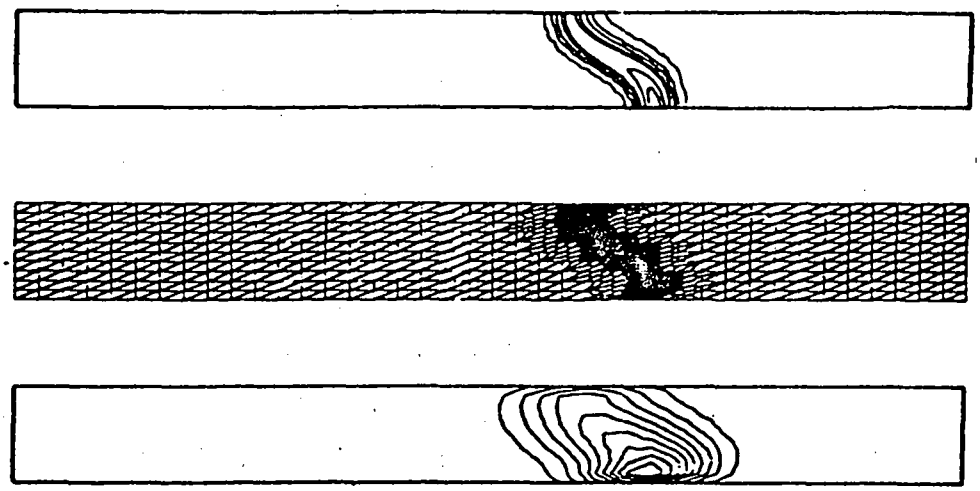

Figure 5.14: Regularisation by mean value
From top to bottom, there are the reaction rate contours, the mesh and the criterion.

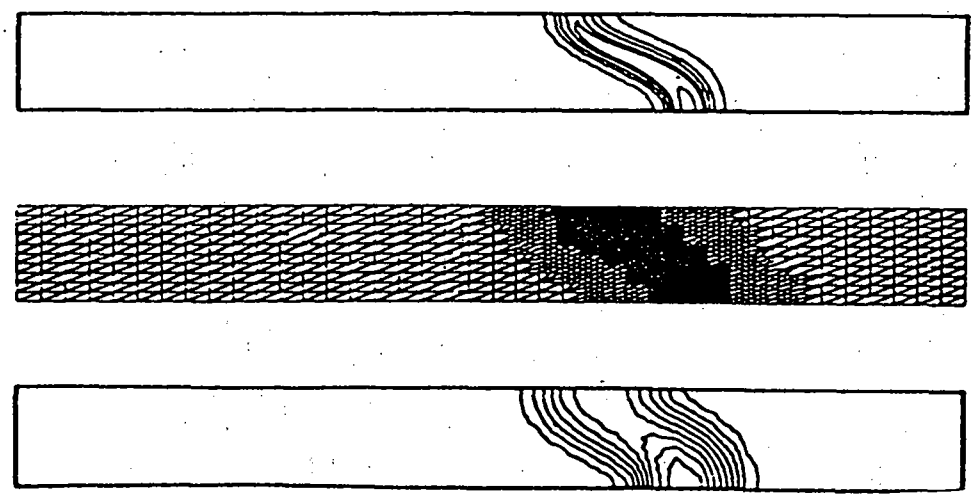

Figure 5.15: Regularisation by Laplacian
See above for legend.

Conclusion and perspectives

Dynamic Mesh refinement/derefinement algorithms provides powerful tools for the simulation of complex reactive unsteady flows presenting disparate scales in time and space. The discretisation thus follows the evolution of the pertinent variables, with a high density of mesh points within critical regions, and a low density of mesh points within zones of quasi-uniform behaviour. The accuracy of the overall result is thus increased, for a relatively low cost in memory and computation time. The criteria for adaptation decision needs careful adjustement to the physical phenmena and the underlying governing equations modelising the phenomena, coupled with the numerical scheme. The use of a finite element approximation allows a precise coupling in this way, using the *a posteriori* finite element error estimators for the scheme, together with normalising physical parameters, and/or physical criteria based on normalised gradient norms of some charcteristic variable. Since the governing equations are non-linear, the evaluation of the discrete error estimator is highly non-trivial.

However, there is no unique golden rule, and many academic tests are necessary to conclude, in order to obtain a sufficiently robust algorithm for such unsteady flows arising in combustion studies. The algorithm has also been adapted successfully to other kinds of unsteady, non-reactive flows [32]. In perspective, a closer coupling of generation principles (Delaunay advancing front algorithms [33]), thus geometrical criteria, to the physical and/or finite element ones are envisaged to maintain more regular discretisations, which although may be bypassed by the simplicity of 2D applications, become mandatory in 3D. Further algorithmic modifications can be made, for instance, the loop over levels can be supressed in ADAPT, and suppression of the hierarchical arborescence can also be acheived [38]. Finally, such algorithms are not adapted to standard Fortran requisites, many recursive commands, conditionnal programming...etc.., but their integration into existing computational programs becomes more straightforward in this way. A closer investigation of the parallelisation of the Mesh generation and Mesh adaptation by refinement/derefinement will be undertaken, in order to evaluate the performances of this valuable tool on new machine architectures.

Acknowledgements

The first author is indepted to Prof. Ryhming at EPFL in Lausanne, and to INRIA/CERMICS for making possible the collaboration *à distance*, since she left INRIA in 1988.

Références

[1] Angrand (F.) et Leyland (P.). - *Une méthode multigrille pour la résolution des équations de Navier-Stokes compressible en deux dimensions par des éléments finis.* - Rapport de recherche n° 593, INRIA[1], Déc. 1986.

[2] Angrand (F.) et Leyland (P.). - *Schéma multigrille dynamique pour la simulation d'écoulements de fluides visqueux compressibles.* - Rapport de recherche n° 659, INRIA, Avr. 1987.

[3] Angrand (F.) et Leyland (P.). - Compressible viscous flow simulation by multigrid methods. *Comp. Meth. Appl. Mech. Eng.*, vol. 75, 1989, pp. 167–183. -

[4] Babuška (I.) et Rheinboldt (W. C.). - Error estimates for adaptive finite element computations. *SIAM J. Numer. Anal.*, vol. 15, n° 4, Août. 1978. -

[5] Babuška (I.), Zienkiewicz (O. C.), Gago (J.) et Arantes e Oliveira (E. R. d.) (édité par). - *Accuracy Estimates and Adaptive Refinements in Finite Element Computations.* - John Wiley & Sons Ltd. 1986. Conference held at Lisbon (Portugal) on June 1984.

[6] Baker (T. J.) et Jameson (A.). - *Multigrid solution of the Euler equations for aircraft configurations.* - Rapport technique n° 84-0093, AIAA, 1984.

[7] Bank (R. E.). - *PLTMG User's Guide.* - Rapport technique, University of California and St Diego, Dept. Mathematics, 1985.

[8] Bank (R. E.) et Sherman (A. H.). - An adaptive multi-level method for elliptic boundary value problems. *Computing*, vol. 26, 1981, pp. 91–105. -

[1] B.P. 93, 06902 Sophia-Antipolis Cedex, FRANCE

[9] Bank (R. E.), Sherman (A. H.) et Weiser (A.). – Refinement algorithms and data structures for local mesh refinement. *In : Scientific Computing*, éd. par Stepelman (R.) et al. IMACS. – Amsterdam, 1983.

[10] Baum (J. D.) et Löhner (R.). – *Numerical simulation of shock-elevated box interaction using adaptive finite-element shock capturing system.* – Rapport technique n° 89-0653, AIAA, 1989.

[11] Benkhaldoun (F.), Fernandez (T.), Larrouturou (B.) et Leyland (P.). – *A Dynamical Adaptive Method Based on Local Refinement and Unrefinement for Triangular Finite-Element Meshes: Preliminary Results.* – Rapport de recherche n° 1271, INRIA. 1990.

[12] Benkhaldoun (F.) et Larrouturou (B.). – Explicit adaptive calculations of wrinkled flame propagation. *Int. J. Num. Meth. Fluids*, vol. 7, 1987, pp. 1147–1158. –

[13] Benkhaldoun (F.) et Larrouturou (B.). – Numerical analysis of the two-dimensional thermo-diffusive model for flame propagation. *Mod. Math. et Anal. Num.*, vol. 22, n° 4, 1988, pp. 535–560. –

[14] Benkhaldoun (F.), Leyland (P.) et Larrouturou (B.). – Dynamic mesh adaption for unsteady nonlinear phenomena - Application to flame propagation. *In : Numerical grid generation in computational fluid mechanics 88*, éd. par Sengupta et al. pp. 977–986. – Miami, 1988.

[15] Brézis (H.). – *Opérateurs maximaux monotones et semi-groupes de contractions dans les espaces de Hilbert.* – North-Holland, 1973, *North-Holland Mathematics Studies*, volume 5.

[16] Brézis (H.). – *Analyse fonctionnelle: théorie et applications.* – Masson, 1983, *Mathématique apliquées pour la maîtrise.*

[17] Ciarlet (P. G.). – *The Finite element method for elliptic problems.* – Amsterdam, North Holland. 1978. *Studies in mathematics and its applications.*

[18] Da Prato (G.) et Tubaro (L.) (édité par). - *Stochastic partial differential equations and applications.* - Springer-Verlag, 1989. Second conference proceedings held at Trento (Italy) on 1-6 February 1988.

[19] Delaunay (B. N.). - Sur la sphère vide. *Bull. Acad. Sciences USSR*, vol. VII: Class. Sci. Math., 1934, pp. 793-800. -

[20] Eriksson (K.). - *Adaptive finite-element methods based on optimal error estimates for linear elliptic problems.* - Chalmers University of Technology, 1987.

[21] Eriksson (K.) et Johnson (C.). - *Adaptive finite-element methods for parabolic problems I: A linear model problem no 31.* - University of Göteborg, Dept. Math., 1988.

[22] Eriksson (K.), Johnson (C.) et Lennblad (J.). - Error estimates and automatic time and space step control for linear parabolic problems. *SIAM J. Num. Anal.*, à paraître en 1990. -

[23] Glowinski (R.). - *Numerical methods for nonlinear variational problems.* - Springer, 1984, *Springer series in computational physics.*

[24] Glowinski (R.), Larrouturou (B.) et Temam (R.) (édité par). - *Numerical simulation of combustion phenomena.* - Springer-Verlag, 1985. Proceedings of the Symposium held at INRIA Sophia-Antipolis (France) on 21-24 May 1985.

[25] Ikeda (T.). - *Maximum Principle in Finite Element Models for Convection-Diffusion Phenomena.* - North-Holland / Kinokuniya, 1983, *North-Holland Mathematics Studies*, volume 76.

[26] INRIA. - *The numerical simulation of compressible Euler flows.* - 1986. GAMM workshop held at Rocquencourt (France) on June 10-13 1986.

[27] Johnson (C.). - Adaptive finite-element methods for diffusion and convection problems. *In: Reliability in Computational Mechanics*, éd. par Oden (J. T.). - 1990. Workshop proceedings held at Austin/Lakeway on october 1989.

[28] Kato (T.). - *Short introduction to perturbation theory for linear operators.* - Springer-Verlag, 1982.

[29] Leclercq (M.-P.). - *Résolution des équations d'Euler par des méthodes multigrilles. Conditions aux limites en régime hypersonique.* - Thèse, Université de St-Etienne, 1990.

[30] Löhner (R.). - An adaptive finite-element scheme for transient problems in CFD. *Comp. Meth. Appl. Mech. Eng.*, vol. 61, 1987, pp. 323–338. -

[31] Löhner (R.), Morgan (K.), Vahdati (M.), Boris (J. P.) et Book (D. L.). - Fem-fct: Combining unstructured grids with high resolution. *Comm. Appl. Num. Meth.*, vol. 4, 1988, pp. 717–730. -

[32] Maman (N.). - *Algorithmes d'adaptation dynamique de maillages en éléments finis. Application à des écoulements réactifs instationnaires.* - Toulouse, Thèse, Université Paul Sabatier, à paraître en 1991.

[33] Mavriplis (D. J.). - *Adaptive Mesh Generation for Viscous Flows Using Delaunay Triangulation.* - ICASE Report n° 88-47, Hampton (Virginia), NASA Langley, 1988.

[34] Nochetto (R. H.), Paolini (M.) et Verdi (C.). - *Local mesh refinements for two-phase Stefan problems in two space variables.* - Pubblic n° 647, Pavia, Instituto di Analisi Numerica, 1988.

[35] Nochetto (R. H.) et Verdi (C.). - An efficient linear scheme to approximate parabolic free boundary problems: error estimates and implementation. *Math. Comp.*, à paraître en 1990. -

[36] Peraire (J.), Vahdati (M.), Morgan (K.) et Zienkiewicz (O. C.). - Adaptive remeshing for compressible flow computations. *J. Comp. Phys.*, vol. 72, 1987, pp. 449–466. -

[37] Pouletty (C.). - *Génération et optimisation de maillages en éléments finis.* - Paris, Thèse, Ecole Centrale des Arts et Manufactures, 1985.

[38] Richter (R.) et Leyland (P.). - *Shock Capturing using Auto Adaptive Finite Elements* Num.Methods for Fluid Dynamics. Avril 1992

[39] Rivara (M.-C.). - Algorithms for refining triangular grids suitable for adaptive and multigrid techniques. *Int. J. Num. Meth. Eng.*, vol. 20, 1984, pp. 745–756. -

[40] Rivara (M.-C.). - Adaptive finite element refinement and fully irregular and conforming triangulations. In Babuška et al. [5], pp. 359–370.

[41] Sivashinsky (G. I.). - Diffusional-thermal theory of cellular flames. *Comb. Sc. Techn.*, vol. 15, 1977, pp. 137–145. -

[42] Ushijima (T.). - Error estimates for the lumped mass approximation of the heat equation. *Memoirs of Numerical Mathematics*, vol. 6, 1979, pp. 65–82. -

[43] Williams (F. A.).- *Combustion Theory.* - Benjamin/Cummings Publ.Co.Inc. 1985.

Contents

List of Figures

Unité de Recherche INRIA Sophia Antipolis
2004, route des Lucioles - B.P. 93 - 06902 SOPHIA ANTIPOLIS Cedex (France)

Unité de Recherche INRIA Lorraine Technopôle de Nancy-Brabois - Campus Scientifique
615, rue du Jardin Botanique - B.P. 101 - 54602 VILLERS LES NANCY Cedex (France)
Unité de Recherche INRIA Rennes IRISA, Campus Universitaire de Beaulieu 35042 RENNES Cedex (France)
Unité de Recherche INRIA Rhône-Alpes 46, avenue Félix Viallet - 38031 GRENOBLE Cedex (France)
Unité de Recherche INRIA Rocquencourt Domaine de Voluceau - Rocquencourt - B.P. 105 - 78153 LE CHESNAY Cedex (France)

EDITEUR
INRIA - Domaine de Voluceau - Rocquencourt - B.P. 105 - 78153 LE CHESNAY Cedex (France)

ISSN 0249 - 6399